

# Giant *Macrocystis* forests

Distribution and trends for the Otago region

*Prepared for Otago Regional Council*

*August 2022*



Prepared by:  
Leigh Tait

For any information regarding this report please contact:

Leigh Tait  
Scientist – Marine Ecology

+64-3-343 7894  
leigh.tait@niwa.co.nz

National Institute of Water & Atmospheric Research Ltd  
PO Box 8602  
Riccarton  
Christchurch 8011

Phone +64 3 348 8987

NIWA CLIENT REPORT No: 2022233CH  
Report date: August 2022  
NIWA Project: ORC22502

Revision	Description	Date
Version 1.0	Final Report	11 August 2022

Quality Assurance Statement		
	Reviewed by:	Chris Woods
	Formatting checked by:	Nic McNeil
	Approved for release by:	Helen Rouse

---

© All rights reserved. This publication may not be reproduced or copied in any form without the permission of the copyright owner(s). Such permission is only to be given in accordance with the terms of the client's contract with NIWA. This copyright extends to all forms of copying and any storage of material in any kind of information retrieval system.

Whilst NIWA has used all reasonable endeavours to ensure that the information contained in this document is accurate, NIWA does not give any express or implied warranty as to the completeness of the information contained herein, or that it will be suitable for any purpose(s) other than those specifically contemplated during the Project or agreed by NIWA and the Client.

# Contents

- Executive summary .....6**
- 1 Introduction .....7**
  - 1.1 Purpose of this report ..... 8
- 2 Methods..... 10**
  - 2.1 Catchment land-use and study regions..... 11
  - 2.2 Remote detection of *Macrocystis* canopies ..... 12
  - 2.3 Satellite derived water quality parameters..... 14
  - 2.4 Data analysis..... 15
- 3 Results..... 16**
  - 3.1 Catchment land-use ..... 16
  - 3.2 In situ data and aerial imagery ..... 16
  - 3.3 Satellite estimates of *Macrocystis* cover and water quality..... 18
  - 3.4 Analysis of trends..... 31
- 4 Summary and recommendations ..... 36**
  - 4.1 Status of *Macrocystis* ..... 36
  - 4.2 Future monitoring..... 37
- 5 Acknowledgements..... 38**
- 6 Glossary of abbreviations and terms ..... 40**
- 7 References..... 41**

**Tables**

- Table 3-1: Total area of floating *Macrocystis* identified with colour matching extractions during April 2016 and March 2017 and differences between years (as hectares and % cover). 17
- Table 3-2: Influence of key parameters on *Macrocystis* coverage as estimated by General Additive Models (GAMs). 32
- Table 3-3: Influence of key parameters on *Macrocystis* coverage at multiple depths as estimated by General Additive Models (GAMs). 35

**Figures**

- Figure 2-1: Bathymetry (m) of the coastal Otago region. 10

Figure 2-2:	Terrestrial land-use types and ecosystems across the Otago region.	12
Figure 2-3:	Timeseries of subtidal <i>Macrocystis</i> densities in situ (Tait 2019) and <i>Macrocystis</i> coverage at the same locations, as estimated by remote sensing (A) and the relationship between in situ densities and remotely estimated coverage (B).	13
Figure 3-1:	Aerial mosaic of <i>Macrocystis</i> cover from Cornish Head in the south to Shag Point in the north.	17
Figure 3-2:	Coverage of <i>Macrocystis</i> between Karitane and Shag Point determined by aerial imagery (A) and satellite imagery (B).	19
Figure 3-3:	Regional variation in remotely sensed water quality products from 2002–20 across the six study regions.	19
Figure 3-4:	Satellite image of <i>Macrocystis</i> cover in the Timaru region including a timeseries of <i>Macrocystis</i> coverage and the influence of sea surface temperature anomalies on coverage.	20
Figure 3-5:	Remotely sensed water quality parameters for the Timaru region.	21
Figure 3-6:	Satellite image of <i>Macrocystis</i> cover in the North Otago region including a timeseries of <i>Macrocystis</i> coverage and the influence of sea surface temperature anomalies on coverage.	22
Figure 3-7:	Remotely sensed water quality parameters for the North Otago region.	23
Figure 3-8:	Satellite image of <i>Macrocystis</i> cover in the Moeraki region including a timeseries of <i>Macrocystis</i> coverage and the influence of sea surface temperature anomalies on coverage.	24
Figure 3-9:	Remotely sensed water quality parameters for the Moeraki region.	25
Figure 3-10:	Satellite image of <i>Macrocystis</i> cover in the Waikouaiti region including a timeseries of <i>Macrocystis</i> coverage and the influence of sea surface temperature anomalies on coverage.	26
Figure 3-11:	Remotely sensed water quality parameters for the Waikouaiti region.	27
Figure 3-12:	Satellite image of <i>Macrocystis</i> cover in the Blue Skin region including a timeseries of <i>Macrocystis</i> coverage and the influence of sea surface temperature anomalies on coverage.	28
Figure 3-13:	Remotely sensed water quality parameters for the Blue Skin region.	29
Figure 3-14:	Satellite image of <i>Macrocystis</i> cover in the Catlins region including a timeseries of <i>Macrocystis</i> coverage and the influence of sea surface temperature anomalies on coverage.	30
Figure 3-15:	Remotely sensed water quality parameters for the Catlins region.	31
Figure 3-16:	Influence of sea surface temperature anomalies on <i>Macrocystis</i> cover between 2016 and 2022.	32
Figure 3-17:	Influence of sea surface temperature anomalies on <i>Macrocystis</i> cover between 2016 and 2022.	33
Figure 3-18:	Influence of sediment loads as determined by the particulate backscatter at 555 nm (BBP) on <i>Macrocystis</i> coverage as separated by region.	33
Figure 3-19:	Interactive effects of TSS and temperature anomalies on <i>Macrocystis</i> cover as determined by generalised additive models (GAM).	34
Figure 3-20:	<i>Macrocystis</i> cover across depths between 2016 and 2022.	35
Figure 4-1:	Remotely sensed water quality products averaged for three zones within the Catlins region, north (near the mouth of the Clutha River), mid (near the Catlins Estuary), and south (near Wapiti (Chaslands) River).	36

Figure 4-2:	Bathymetry of the Otago Coast from the Otago Peninsula to the Moeraki Peninsula.	37
Figure 4-3:	Candidate regions of coastal <i>Durvillaea</i> habitats for high-resolution aerial monitoring.	38

## Executive summary

Kelp forests support some of the highest levels of biodiversity in Aotearoa New Zealand. They support: marine food-webs; important recreational, commercial, and cultural fisheries; and are increasingly viewed for their pharmaceutical, nutritional and carbon capture potential. There is, however, anecdotal evidence of reductions in *Macrocystis* forests in Southern Otago and empirical evidence of retractions at the national level. Marine heatwaves are a major stressor to kelp forests globally, but local stressors such as sediment input have been shown to exacerbate the consequences of climatic events on kelp forests.

Otago Regional Council (ORC) has regulatory obligations under the Resource Management Act 1991 and the New Zealand Coastal Policy Statement, Policy 11, to protect indigenous biological diversity in the coastal environment. The purpose of this report is to support ORC in meeting these obligations by assessing the status of kelp forests and informing monitoring of kelp forest habitats that will enable management decisions to better include outcomes for marine ecosystems. This information will be used to inform an effective coastal plan and enable data-driven decisions that identify and mitigate potential impacts caused by terrestrial land-use management regimes.

Here, I apply satellite remote sensing to establish baseline information on the cover of the giant kelp *Macrocystis pyrifera* (hereafter referred to as *Macrocystis*) and key water quality parameters across regions exposed to varying land-use regimes. I examine the implications of region-wide gradients of key stressors (e.g., sedimentation) on the coverage of *Macrocystis*, as well as temporal shifts in coverage as related to seasonal trends (e.g., temperature) and extreme events (e.g., marine heatwaves). Results show that water temperature is a major driver of reductions in *Macrocystis* cover as observed during two marine heatwaves (summer 2017–18 and summer 2012–22). While there was little evidence of sediment driven reductions of *Macrocystis* cover within regions, there were major differences in *Macrocystis* coverage across regions exposed to varying sediment concentrations.

Using national scale bathymetric layers, I examined the influence of water quality parameters on the potential depth distribution of *Macrocystis*. Results revealed that both warmer temperatures and elevated suspended sediments compress the habitable depth range for *Macrocystis* and indicate maximum depth ranges of between 25–35 m. These results are used to inform future monitoring of populations that are likely to be highly susceptible to changes in temperature and sedimentation regimes, and thus likely to provide responsive indicators of change.

Assessment of gradients of sedimentation and relative land-use informed monitoring strategies for kelp species (*Durvillaea* spp. and *Macrocystis*). I provide recommendations for the establishment of long-term monitoring which uses *Macrocystis* and *Durvillaea* as indicators of ecosystem health across gradients of exposure to land-use pressure. This information will be used to plan field campaigns of aerial imagery mapping of discrete rocky headlands for *Durvillaea* and calibration of remote monitoring of *Macrocystis* across the Otago region.

# 1 Introduction

Kelp dominated coastal rocky reef ecosystems are critically important to Aotearoa New Zealand but are in decline in response to multiple stressors including marine heatwaves, and shading effects of coastal sedimentation (Tait 2019; Thomsen et al. 2019; Blain et al. 2021; Tait et al. 2021). The status of coastal reef ecosystems is often assumed rather than known because they are difficult to access, but the impacts are real – loss of productivity, broken trophic linkages and impaired ecosystem functioning. These impacts are often associated with degradation of kelp forests that underpin these ecosystems (Rogers-Bennett and Catton 2019; Tait et al. 2021).

The biogenic habitats of large macroalgae are nurseries for fishes and invertebrates of cultural, recreational, and economic importance (Layton et al. 2020). Their productivity contributes directly to 40% of the biomass of coastal fishes (Udy et al. 2019); at stake are hundreds of millions of dollars of gross domestic product (GDP) from pāua, kōura, and inshore fisheries. Large macroalgae are a key indicator of wider ecological health, and unlike many other ecosystem components, are conspicuous and remain fixed to a location. For these reasons they integrate and reflect many of the stressors affecting rocky reef habitats (D’Archino and Piazzini 2021).

Giant kelp, *Macrocystis pyrifera* (hereafter referred to as *Macrocystis*), is one of the fastest growing photosynthetic organisms globally, and is a key contributor to carbon fixation and habitat provision for temperate marine ecosystems across a large extent of the world’s temperate coastlines (Schiel and Foster 2015; Miller et al. 2018). Recent studies have revealed that *Macrocystis* and other large kelps have had retractions in the northern hemisphere (Arafeh-Dalmau et al. 2019; Rogers-Bennett and Catton 2019), often in response to combined physical and trophic interactions (Ling et al. 2009; Rogers-Bennett and Catton 2019). In southern Australia, *Macrocystis* has experienced massive retractions, and is nearing functional extinction in some regions in response to oceanographic shifts that have increased larval delivery of a key herbivorous urchin, decreased nitrogen concentrations and high seawater temperatures (Mabin et al. 2019; Butler et al. 2020). A study of the *Macrocystis* populations along the Otago coast show that a key driver of *Macrocystis* health is turbidity and reduced light availability (Tait 2019). More recent research (Tait et al. 2021) has revealed that the 2017–18 marine heatwave had significant negative effects on *Macrocystis* nationwide, including the Otago Coast, with water clarity interacting to further reduce coverage of *Macrocystis*.

Southern bull kelp, dominated by three species *Durvillaea antarctica*, *Durvillaea poha* and *Durvillaea willana* (hereafter collectively referred to as “*Durvillaea*”), are some of the largest macroalgal species and in New Zealand are represented by several native and endemic species. Like *Macrocystis*, *Durvillaea* are important contributors to a range of vital ecosystem services. Unlike *Macrocystis*, however, these species inhabit rocky reefs along the coastal fringe, are tolerant of very heavy wave exposure and are therefore widely distributed along New Zealand’s southern coastlines (from Wairarapa/Wellington to the Sub-Antarctic Islands). Like *Macrocystis*, *Durvillaea* have proved highly vulnerable to marine heatwaves (Tait et al. 2021; Thomsen et al. 2019, 2021). Less is known globally about the stressors affecting *Durvillaea* species, but while light can be less limiting to macroalgae higher up the shore, sediments can still have a negative influence on macroalgal populations (Alestra et al. 2014; Schiel and Gunn 2019).

*Macrocystis* and *Durvillaea* both occur throughout the Otago Region. However, the Otago Peninsula represents a key breakpoint for populations of these species, a product of the protection that Otago Peninsula provides from large swells originating in the Southern Ocean. *Macrocystis* forests flourish

along the coast north of the Otago Peninsula thanks to the protection from a large proportion of southerly swells (Tait 2019), while *Durvillaea* dominates the highly exposed headlands and rocky reef south of the Otago Peninsula.

New Zealand has experienced some of its most intense marine heatwaves in its climate record in the past five years (Salinger et al. 2019) causing localized extinctions of *Durvillaea* (Thomsen et al. 2019), and declines in *Macrocystis* across mainland New Zealand (Tait et al. 2021). Rapid rates of land-use change associated with agriculture and urbanisation have dramatically altered the land-water interface globally, including in New Zealand, where rates of sedimentation have increased as a result (Goff 1997). Proximity of *Macrocystis* forests to sources of sediments greatly affects the demography of populations which exhibit a poor rate of conversion from juvenile sporophytes to adult plants reaching the surface (Tait 2019). Likewise, deposited sediments can inhibit the settlement of propagules of both *Durvillaea* and *Macrocystis*. Sediment accretion and reef burial is also possible (Tait 2019), yet these processes are some of the least understood consequences of sediment inputs. The impacts of land-management regimes, particularly the delivery of sediments to the marine environment, requires consistent and broad-scale monitoring to understand the impacts of terrigenous sediments, and the potential management and intervention measures which will improve outcomes for marine ecosystems. Otago's coastline is home to a wide range of diverse and unique ecosystems. These ecosystems are biodiversity hotspots with deep sea canyons, bryozoan reefs, rhodolith beds, gravel/boulder fields and kelp forests. This diversity of habitats and the nutrient rich currents such as the Southland and Sub-Antarctic currents create the conditions that make Otago's marine life highly diverse with many iconic species (e.g., pāua, kōura, blue cod, sperm whales, albatross, yellow eyed penguins, and sea lions). Among these ecosystems, the importance of kelp forests along Otago's Coast is reflected in their designation as 'marine significant ecological areas' in Department of Conservation (2010).

Otago Regional Council (ORC) has regulatory obligations under the Resource Management Act 1991 (RMA) and the New Zealand Coastal Policy Statement, Policy 11, to protect indigenous biological diversity in the coastal environment. Regional councils must provide for the preservation of natural character (which includes an ecological element) (RMA, Section 6a) and protection of indigenous vegetation and fauna (RMA, Section 6c). Otago's jurisdiction (Regional Policy Statement and Regional Plan: Coast) runs from mean high-water spring (MHWS) out to 12 nautical miles. Our proposal is to support ORC in meeting these obligations by mapping and monitoring kelp forest habitats/ecosystems. This will provide information for the creation of an effective coastal plan and enable informed management decisions to identify and mitigate the impacts of potential stressors on kelp forests such as sedimentation from land.

## 1.1 Purpose of this report

This report represents "Phase 1" of a multi-year programme that will provide baseline knowledge and provide guidance for ongoing monitoring of Otago's coastal marine ecosystems. In Phase 1, I will review several sources of information to select sites for passive and active monitoring. Monitoring will consider *Macrocystis* and *Durvillaea* habitats separately and will select multiple sites of each habitat across gradients of potential stress, particularly associated with land-use scenarios. The sources of information I will utilise include:

- technical reports and grey literature (e.g., reports for regional councils)
- peer-reviewed scientific literature
- satellite information.

As part of the review, I will establish qualitative and quantitative information about the abundance, distribution, and status of *Macrocystis*, the relative status of terrestrial catchments, and broad estimates of water quality parameters across several regions of the Otago Coast. Moderate resolution marine bathymetry will also be incorporated to explore the depth distribution in regions exposed to varying turbidity. This will provide key information to inform upcoming in situ monitoring campaigns.

I will use multiple satellite platforms to detect and quantify *Macrocystis* forests across the Otago region using methods developed by NIWA (Tait et al. 2021). Passive remote sensing has been widely used for monitoring marine ecosystems (Bell et al. 2020; Mora-Soto et al. 2020) and the widely accepted approach generally computes vegetation indices based on measurements of near infrared electromagnetic radiation (ideally at red edge bands; Timmer et al. 2022). These indices detect vegetation not occluded by overlying water, giving a direct measurement of only the floating portion of macroalgal canopies. Because the approach is limited to the detection of surface canopies, these datasets are unable to integrate the full population dynamics of *Macrocystis* and give no insight into the presence of subsurface *Macrocystis* forests.

ORC wish to establish an environmental baseline for these key components of their rocky reef ecosystems. Here, I review information about *Macrocystis*-dominated coastal marine ecosystems in Otago, provide updated time-series analysis with satellite imagery and identify the influence of water quality parameters on kelp forest coverage. Using this analysis I will provide recommendations on the monitoring approach for the next phase of this project, including identifying key populations, regions, and methods that will help calibrate and validate remotely sensed metrics.

## 2 Methods

*Macrocystis* inhabits subtidal reefs down to approximately 20–25 m depth in the Otago region (Tait 2019). While *Macrocystis* populations that inhabit shallow depths (e.g., 5–10 m) are regularly visible from aerial or satellite imagery, deeper populations may not be. In this study I examine the coverage of *Macrocystis* broadly across all depths, however, I also explore the detection of surface canopies at different depths (as defined by a national bathymetric dataset; NIWA; Figure 2-1). I explore the variability of the coverage of *Macrocystis* across depth ranges to help inform in situ validation campaigns.

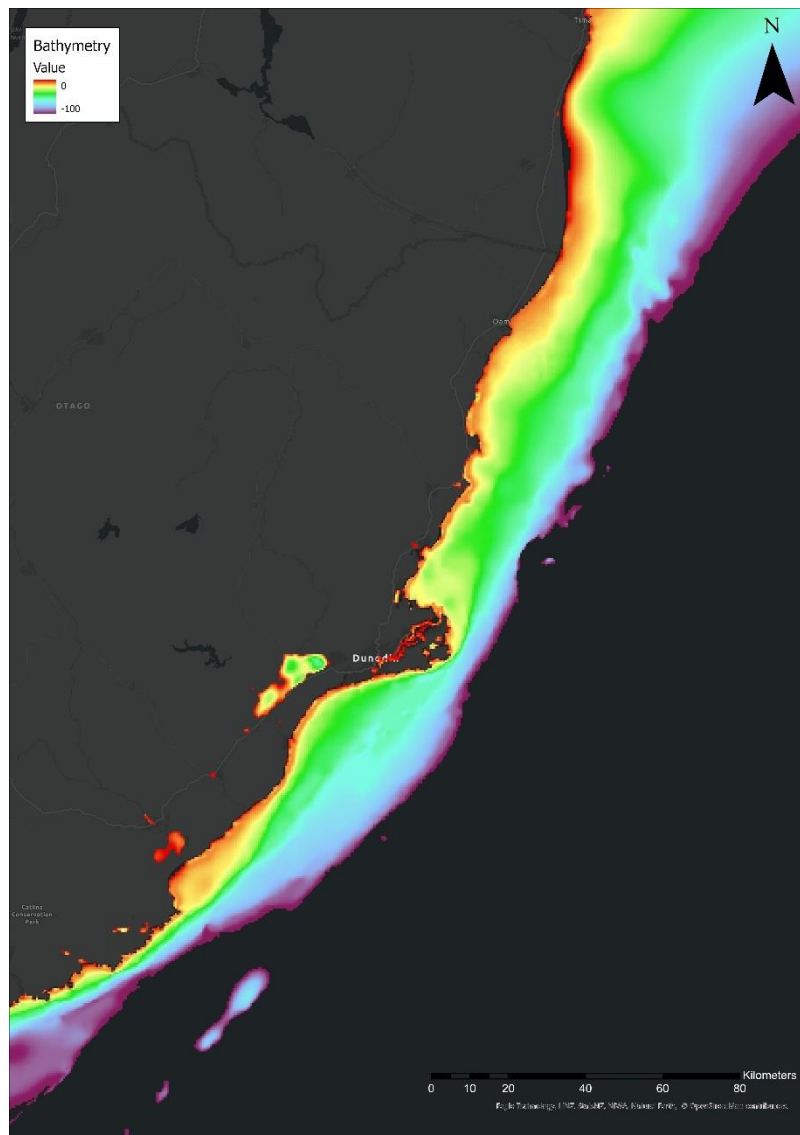


**Figure 2-1:** Bathymetry (m) of the coastal Otago region. Bathymetric layer is masked to display depths from 0 to 100m.

*Durvillaea* inhabit exposed rocky reef platforms in the intertidal and shallow subtidal zone. Several years of combined in situ and aerial monitoring on several headlands near the Otago Harbour have been completed on behalf of Port Otago Ltd (Tait 2020). These will form the basis of a 25-year programme to monitor these habitats to determine negative consequences of sediment disposal at the Heyward dredge spoil grounds (offshore from Hayward Point; Tait 2020). Although satellite-

based remote sensing of these populations is challenging due to the narrow zone inhabited by these species, I will use existing data to provide guidance on the design of a monitoring programme for these habitats, particularly relating to the Catlins region.

I explore the distribution of *Macrocystis* with the aid of several datasets, particularly aerial and in situ datasets collected on behalf of Port Otago Ltd during the “Project Next Generation” capital dredging programme (Tait 2018), and for consenting of long-term maintenance dredging (Tait 2020). I present information collected during these monitoring campaigns for Port Otago to summarise the best available knowledge of these marine forests, provide guidance for ongoing monitoring and to provide context for remote monitoring techniques. The methodology implemented for these surveys can be found in Tait (2018) and Tait (2020). Furthermore, I leverage remote sensing techniques developed by Tait et al. (2021) to examine trends in *Macrocystis* cover from 2016 to 2022.

## 2.1 Catchment land-use and study regions

Broadly defined terrestrial habitat classes were downloaded from (<https://Iris.scinfo.org.nz/layer/95415-basic-ecosystems/>). The data provide high resolution (e.g., 15 m<sup>2</sup>) estimates of land-use based on satellite products integrated between 2002–12. The 17 habitat classes defined in the original datasets (Dymond et al. 2012) were then collapsed into eight land-use types including: urban; coastal ecosystems; alpine ecosystems; water (fresh); agriculture; tussock/grassland/scrubland; exotic forest; and native forest. Each marine region was chosen based on natural breaks such as headlands and exposure to terrestrial catchments (Figure 2-2). The study zones used to assess regional cover of *Macrocystis* were chosen based on natural geological breaks and exposure to various terrestrial and freshwater catchments.

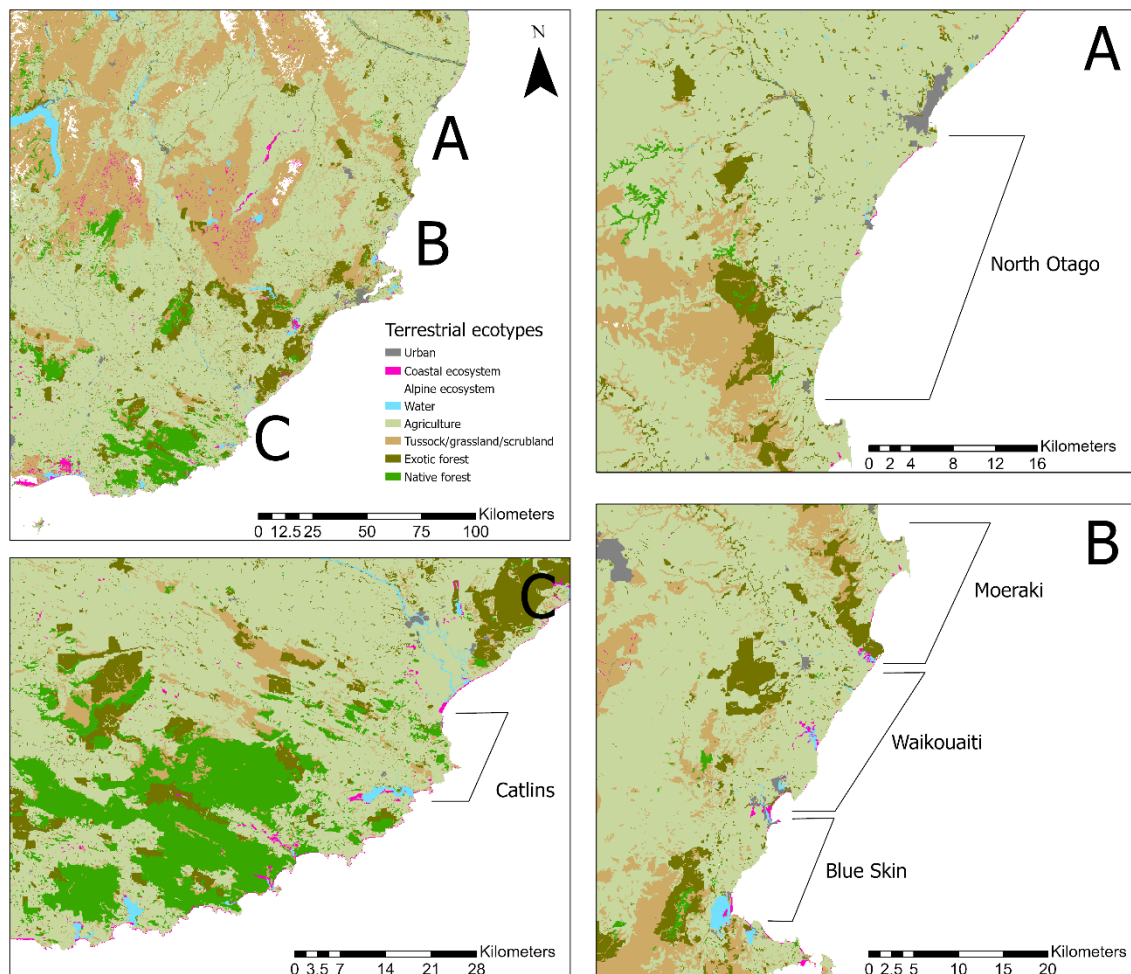


**Figure 2-2: Terrestrial land-use types and ecosystems across the Otago region.** Locations and extents of regions used to estimate *Macrocystis* coverage are shown in each subregion (A, B, and C).

## 2.2 Remote detection of *Macrocystis* canopies

Surface canopies of *Macrocystis* were assessed using Sentinel-2 satellite imagery (resolution = 100 m<sup>2</sup>) between December 2015 and May 2022 (Copernicus Sentinel-2A data 2015–2022). Six focal regions spanning the Southern Canterbury<sup>1</sup> and Otago coastline were chosen, relating to key populations of *Macrocystis* (Hay 1990) and geological breaks. *Macrocystis* cover (m<sup>2</sup>) was calculated from the number of pixels with detectable vegetation multiplied by the pixel area (100 m<sup>2</sup>). Data were filtered, masked, and downloaded using Google Earth Engine (Gorelick et al. 2017). Although the timing of satellite capture was not synced to tidal cycles (with a tidal range of ca. 2 m in most of our study region), with potential implications for the visible extent of canopies, remote sensing studies of *Nereocystis luetkeana* (Finger et al. 2021) and *Macrocystis* (Butler et al. 2020) show that variation in coverage was not particularly sensitive to tidal height.

The Normalized Difference Vegetation Index (NDVI) and the Normalized Difference Water Index (NDWI) were calculated from the visible light and “red-edge” (Timmer et al. 2022) bands of the

<sup>1</sup> Timaru, is within the jurisdiction of Environment Canterbury. However, populations of *Macrocystis* occur at this location and are exposed to generally high sediment loads. Including this site in this analysis provides a useful comparison to the Otago region.

Sentinel-2 constellation. Specifically, the bands B3 (559.8 nm) and B8 (832.8 nm) were used to calculate NDWI and B4 (664.6 nm), and B5 (710.0 nm) was used to calculate the “red-edge” vegetation index. To differentiate *Macrocystis* from other features, a series of masking and filtering procedures was performed. First, monthly near cloud-free images were selected by using quality control bands (Sentinal-2 QA band 60). The acceptable percentage of cloud cover was set to 10%. The coastline and offshore islands were masked by an elevation layer to remove all land-based pixels. The thresholds of the NDVI were set to >0.01 slightly more conservative than the threshold set for detection of *Macrocystis* by Mora-Soto et al. (2020), but less than thresholds for seagrass (0.2; Calleja et al. 2017), and the threshold of NDWI was set to <0.2 based on detection results of well-studied forests (Tait 2019). Finally, the monthly cover (when appropriate imagery was available) of *Macrocystis* was estimated within each of six polygons which cover the entirety of the six distinct areas (Figure 2-2; note, figure excludes the Timaru region).

Kelp detection results were tested against in situ subtidal densities of *Macrocystis* (Tait 2019). In situ subtidal population surveys (Tait 2019) partially spanned the satellite time-series and allowed near-direct comparisons. I compare the densities of mature *Macrocystis* measured at eight subtidal sites at 8–11 m depth to satellite estimated coverage in a 100 × 100 m polygon centred at each subtidal site. Comparisons between subtidal densities of *Macrocystis* and remote estimates revealed a strong positive linear relationship, but also some variation between subtidal densities and the coverage of surface canopies (Figure 2-3).

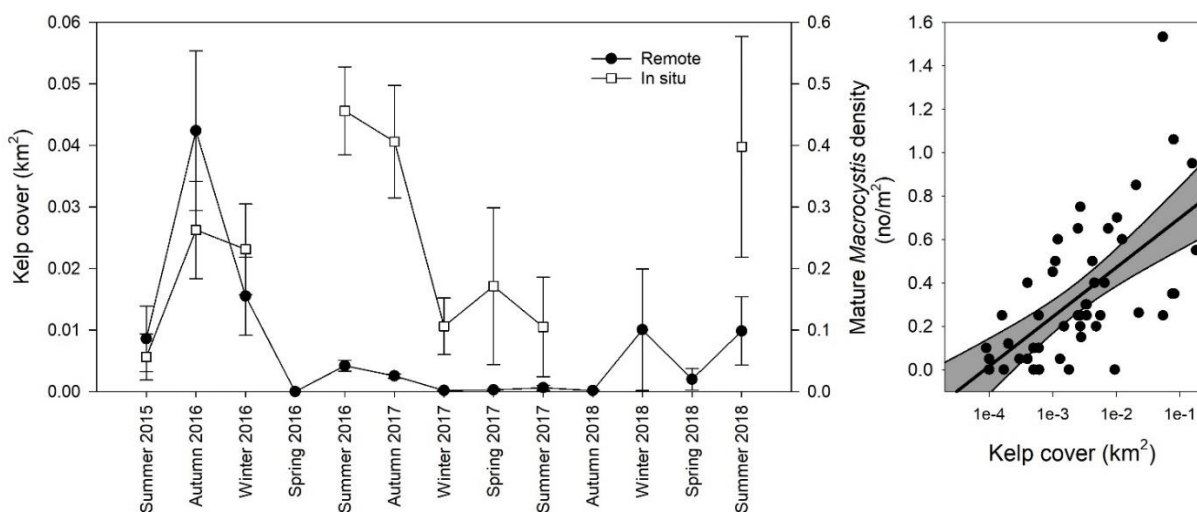


**Figure 2-3: Timeseries of subtidal *Macrocystis* densities in situ (Tait 2019) and *Macrocystis* coverage at the same locations, as estimated by remote sensing (A) and the relationship between in situ densities and remotely estimated coverage (B).** Linear regression (B) had a significant positive slope ( $t= 5.8$ ,  $p<0.0001$ ) and reasonable fit ( $R^2 = 0.34$ ). Kelp cover x-axis log transformed (B). Although the method does not provide a specific canopy area per pixel, instead assuming 100% canopy coverage within pixels, similar NDVI based vegetation detection methods have been shown to provide an effective proxy for *Macrocystis* extent and abundance (Cavanaugh et al. 2010; Nijland et al. 2019). This provides a standardized method for identifying the presence and relative extent of *Macrocystis* forests to identify spatio-temporal trends in relation to key environmental parameters (Butler et al. 2020).

## 2.3 Satellite derived water quality parameters

Key metrics of water quality, particularly those relating to water temperature, water visibility and light availability, were extracted from SCENZ (Seas, Coasts and Estuaries, New Zealand) using novel algorithms specifically tuned for the New Zealand coastal region (Pinkerton et al. 2021). Here I used the chlorophyll-*a*, KPAR (K<sub>d</sub> for Photosynthetically Active Radiation [PAR] wavelengths), total suspended solids (TSS) and sea surface temperature (SST). Each parameter was extracted across polygons 1 × 10 km wide placed c. 1 mkm from the coast for each region. Monthly means were extracted from SCENZ from 2002–20 for each pixel within the coastal polygons and the mean calculated for each polygon (i.e., averaged across all pixels).

### 2.3.1 Sea surface temperature

SST time-series were obtained from the MODIS-Aqua measurements using the SeaDAS v7.2 default 'sst' product which is derived from measurements of long-wave (11–12 μm) thermal radiation (NASA 2018). SST products at 1 km were subsampled to 500 m to improve resolution of the narrow channels over time using bilinear interpolation. Accuracy of SST is likely to be high; Pinkerton (2017) found that, in a similar New Zealand region (Manukau Harbour), these SST observations closely followed in situ measurements of surface temperature ( $R^2 = 0.924$ ,  $n = 172$ ). Further validation came from a comparison between MODIS-Aqua SST and OISST (Optimum Interpolation Sea Surface Temperature, version 2, Reynolds et al. 2002) for the New Zealand coast (Pinkerton et al. 2019;  $r^2 = 0.972$ ,  $n = 256,687$ ).

### 2.3.2 Chlorophyll-*a*

Chlorophyll-*a* concentration (chl-*a*) was estimated using satellite measurements of ocean colour from the Moderate Resolution Imaging Spectrometer on the Aqua satellite (MODIS-Aqua)—owned and operated by the US National Aeronautics and Space Administration (NASA 2018). I used the Quasi-Analytical Algorithm (QAA) algorithm (Lee et al. 2002, 2009) to estimate particulate backscatter at 555 nm [bbp(555)] and phytoplankton absorption at 488 nm [aph(488)]. Phytoplankton absorption was converted to an estimate of chl-*a* using the chl-specific absorption coefficient,  $aph^*(488)$ . The value of  $aph^*(488)$  can vary seasonally and spatially, relating to different phytoplankton species (with varying cell physiology and pigments), different phytoplankton cell sizes, and the light environment (Kirk 2011). Here, I used an average of values found for oceanic phytoplankton (Bricaud et al. 1995; Bissett et al. 1997), and measurements in the lower reaches of New Zealand rivers and estuaries. I blended the QAA-chl-*a* and the MODIS-default chl-*a* product (NASA, 2018) using a logistic-scaling of bbp(555) (Pinkerton et al. 2018).

### 2.3.3 Sediment loading

The diffuse downwelling attenuation coefficient in the Photosynthetically Available Radiation (PAR range, 400–700 nm),  $K_d$  ( $m^{-1}$ ) was used as our measure of water clarity. Values of  $K_d$  were estimated from MODIS-Aqua measurements of ocean colour, processed to inherent optical properties using the QAA algorithm (Lee et al. 2002, 2009) following the methodology of Pinkerton et al. (2018). From these IOPs, I estimated the diffuse attenuation coefficient in the PAR range as Lee et al. (2005). The satellite-derived attenuation coefficient was mapped at a nominal resolution of 500 × 500 m and projected to a transverse Mercator grid. The temporal resolution of the product for the study region is 1–2 measurements daily. Values of  $K_d$  were extracted from the dataset around *Macrocystis* forests and averaged monthly to provide a dataset with low quantities of missing data (Pinkerton et al. 2018).

## 2.4 Data analysis

Monthly estimates of *Macrocystis* coverage from five polygons within each region (Timaru, North Otago, Moeraki, Waikouaiti, Blue Skin, and Catlins) were averaged and aligned with monthly means of SST, TSS,  $K_d$ , and chl- $a$  estimated at the zone level (12 zones within four regions). Given variation in cloud cover during satellite passes, variation in imagery availability resulted in variable sample numbers across regions.

The effects of monthly maximum SST, temperature anomaly, water clarity (as defined by the light attenuation coefficient  $K_d$ ), TSS, and chl- $a$  concentration (as a surrogate for nutrient availability) on *Macrocystis* cover were analyzed with Generalized Additive Models (GAMs) using the “R” package “mgcv.” Assumptions of normality (Q-Q plot), homogeneity of variance (Levene’s Test), as well as “concurvity” for general additive model analysis (an estimate of redundancy among explanatory variables) were used to check that model assumptions were met. GAM models were fitted with “cr” (cubic regression) splines, using a k-value of six (i.e., the number of “knots” denoting the complexity of the non-linear fit), and the distribution family gaussian. Selection procedures were implemented to penalize and remove factors with poor explanatory power. The final model included mean monthly SST anomalies,  $K_d$ , TSS, chl- $a$ , maximum significant wave height and the two-way interaction between water clarity and temperature anomalies.

## 3 Results

### 3.1 Catchment land-use

The Timaru region (not shown) was dominated by urban and agricultural habitats but is also north of several major rivers (e.g., Waitaki), the outputs of which are transported northwards via the Southland Current (Sutton 2003). The North Otago region is also dominated by agriculture, and urban areas, but has smaller freshwater catchments than the Timaru region (Figure 2-2 A). The Moeraki region, dominated by the Moeraki Peninsula, has a high proportion of exotic forests and few major rivers (Figure 2-2 B). The Waikouaiti region is further into the lee of the Otago Peninsula, the land-use is dominated by agriculture and the three nearby major freshwater catchments (Shag, Pleasant, Waikouaiti) have some regions of intact wetland habitats (Figure 2-2 B). The Blue Skin region is well within the lee of the Otago Peninsula, with a catchment of land-use dominated by agriculture, exotic forest, native forest, and scrubland (Figure 2-2 B). The Catlins region is more exposed than the other regions due to the prevailing south-westerly wind and swell, but in the lee of small and large headlands (e.g., Nugget Point) populations of *Macrocystis* exist. The land-use of the Catlins includes the greatest native forest coverage of all regions (Figure 2-2 C). At the northern extent of the Catlins, one of New Zealand's largest rivers, the Clutha River, reaches the coast. The Clutha River and the gradient of native forest cover further south are expected to create a natural gradient of sediment exposure from north to south.

### 3.2 In situ data and aerial imagery

Aerial imagery collected during early April 2016 and late March 2017 showed extensive *Macrocystis* forests covering a large proportion of the coastline from Cornish Head to Shag Point. Classification of *Macrocystis* using colour matching algorithms were used on raw orthomosaic images (Figure 3-1). Overall patterns revealed the occurrence of large continuous patches of *Macrocystis* in the southern extent through to Bobby's Head (small rocky outcrop approximately in the centre of the zone), but north of this point are increasingly dominated by smaller patchy *Macrocystis* forests.

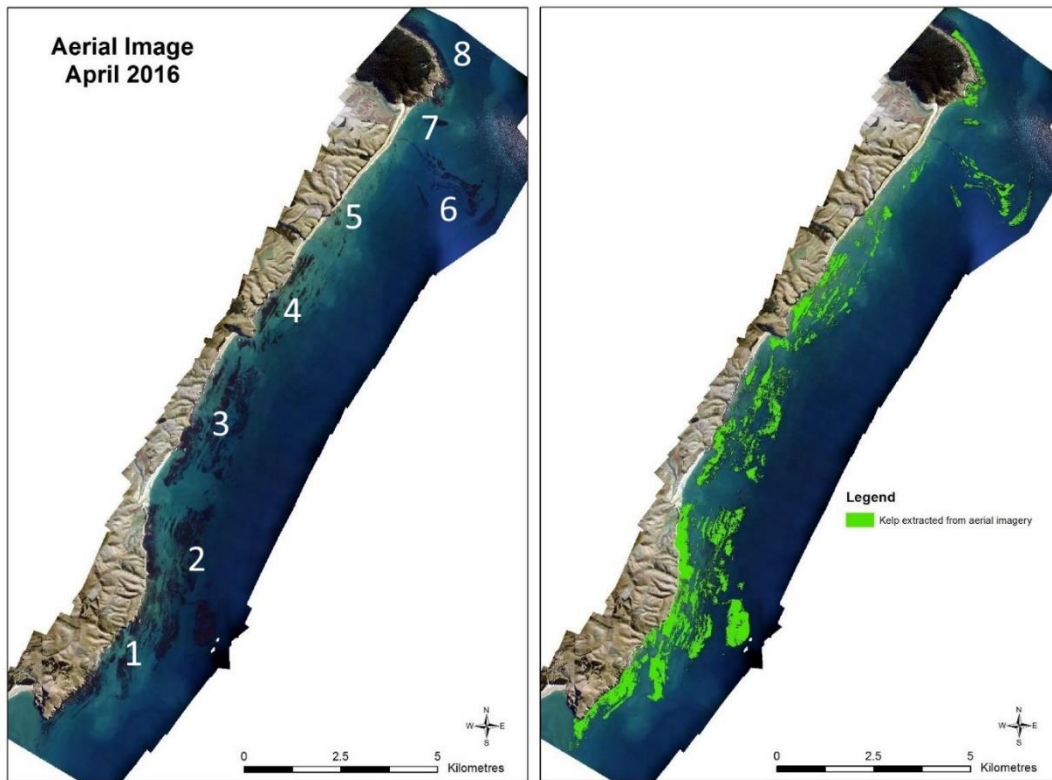


**Figure 3-1:** Aerial mosaic of *Macrocyctis* cover from Cornish Head in the south to Shag Point in the north. Numbers indicate regions where total coverage of *Macrocyctis* was summed (see Table 3-1).

**Table 3-1:** Total area of floating *Macrocyctis* identified with colour matching extractions during April 2016 and March 2017 and differences between years (as hectares and % cover). Total area shown in hectares (10,000 m<sup>2</sup>) and aerial imagery for two regions (2 and 6) was incomplete for the March 2017 sampling.

Region	Total area 10,000 m <sup>2</sup> (April 2016)	Total area 10,000 m <sup>2</sup> (March 2017)	Change 2016–17 (10,000 m <sup>2</sup> )	Change 2016–17 (%)
1	233.5	85.1	-148.4	-64%
2	138.7	35.0	-103.7	-75%
3	116.8	127.3	10.6	9%
4	85.3	30.6	-54.7	-64%
5	23.8	12.4	-11.5	-48%
6	39.9	2.7	-37.2	-93%
7	11.6	3.5	-8.0	-69%
8	16.8	10.0	-6.8	-41%
<b>TOTAL</b>	<b>666.4</b>	<b>306.6</b>	<b>-359.7</b>	<b>-54%</b>

Relative changes in broad-scale *Macrocyctis* coverage estimated by aerial imagery showed that April 2016 had far greater surface *Macrocyctis* abundance than March 2017 (Table 3-1). Only region 3

showed a positive gain in *Macrocystis* cover from April 2016 to March 2017 (increase by 9%). All other sites (excluding those for which an overlapping image was not captured in March 2017), show a 41–69% decline in surface *Macrocystis* coverage. Although it is possible that extraction of colour signals associated with *Macrocystis* was affected in the nearshore due to higher turbidity, there was a noticeable reduction in *Macrocystis* bed size across the onshore to offshore turbidity gradient from 2016 to 2017.

### 3.3 Satellite estimates of *Macrocystis* cover and water quality

#### 3.3.1 Regional trends in *Macrocystis* cover and water quality

Comparisons between aerial imaging (manned fixed-wing aircraft) taken in April 2016 over the region from Karitane to Shag Point and satellite images over the same region revealed very close overlap in *Macrocystis* coverage (Figure 3-2). Although the coverage calculated from aerial imagery was higher (666 ha) than satellite estimates (402 ha), all the major *Macrocystis* forests were well described by the lower resolution satellite images. Disagreement in the final values is largely a result of the higher resolution of aerial imaging, the selection of low tide conditions, and variability in the visibility of *Macrocystis* below the surface.

Remotely sensed water quality products, particularly those relating to water clarity, varied considerably between regions (Figure 3-3). PAR attenuation ( $K_d$ ) was very high in the Timaru region and was elevated in the North Otago and Catlins regions but was far lower and less variable in the Moeraki, Waikouaiti and Blue Skin Bay regions. Mean SST was relatively similar between regions, although Timaru and the Catlins experienced a greater range of temperatures. TSS were notably higher in the Timaru region compared to all other regions, although both North Otago and the Catlins regions both had elevated TSS compared to Moeraki, Waikouaiti and Blue Skin Bay. Chl-*a* showed a similar trend, but the differences between sites was less pronounced.

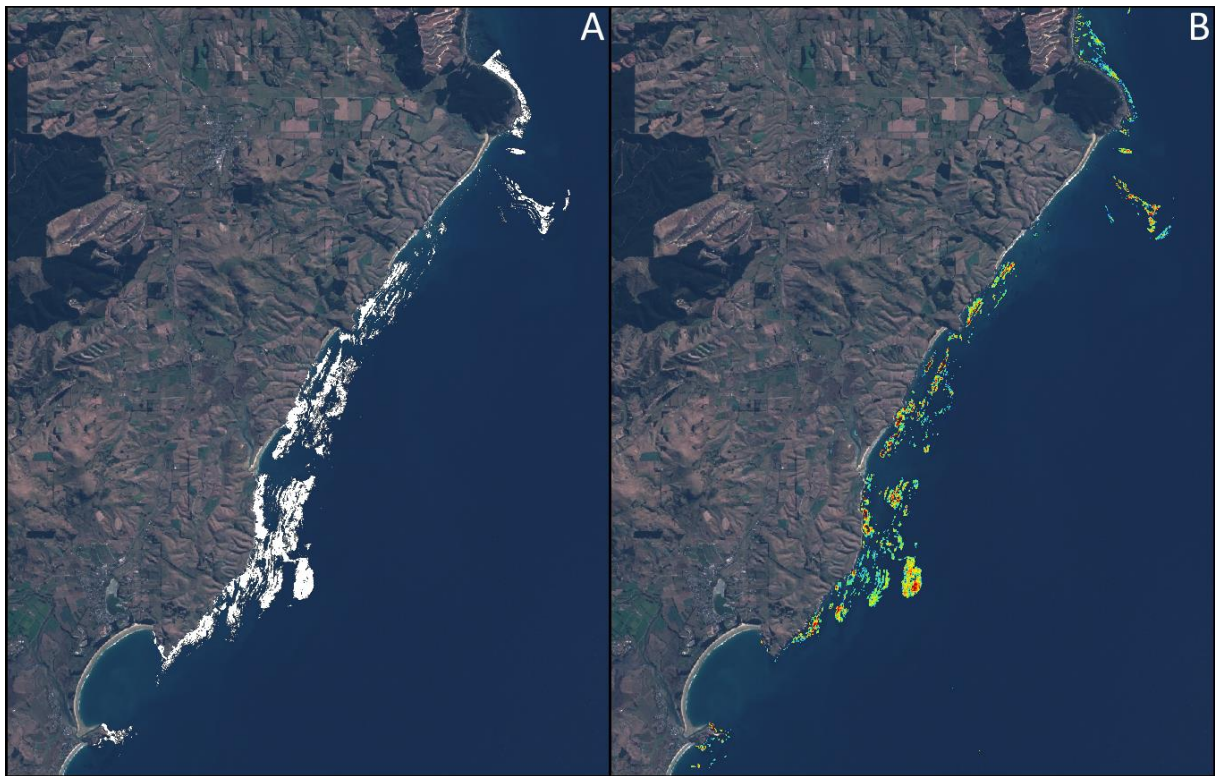


**Figure 3-2: Coverage of *Macrocytis* between Karitane and Shag Point determined by aerial imagery (A) and satellite imagery (B).** Aerial imagery was analysed using machine learning techniques, while satellite imagery is filtered using vegetation indices that rely on “red-edge” wavelengths.

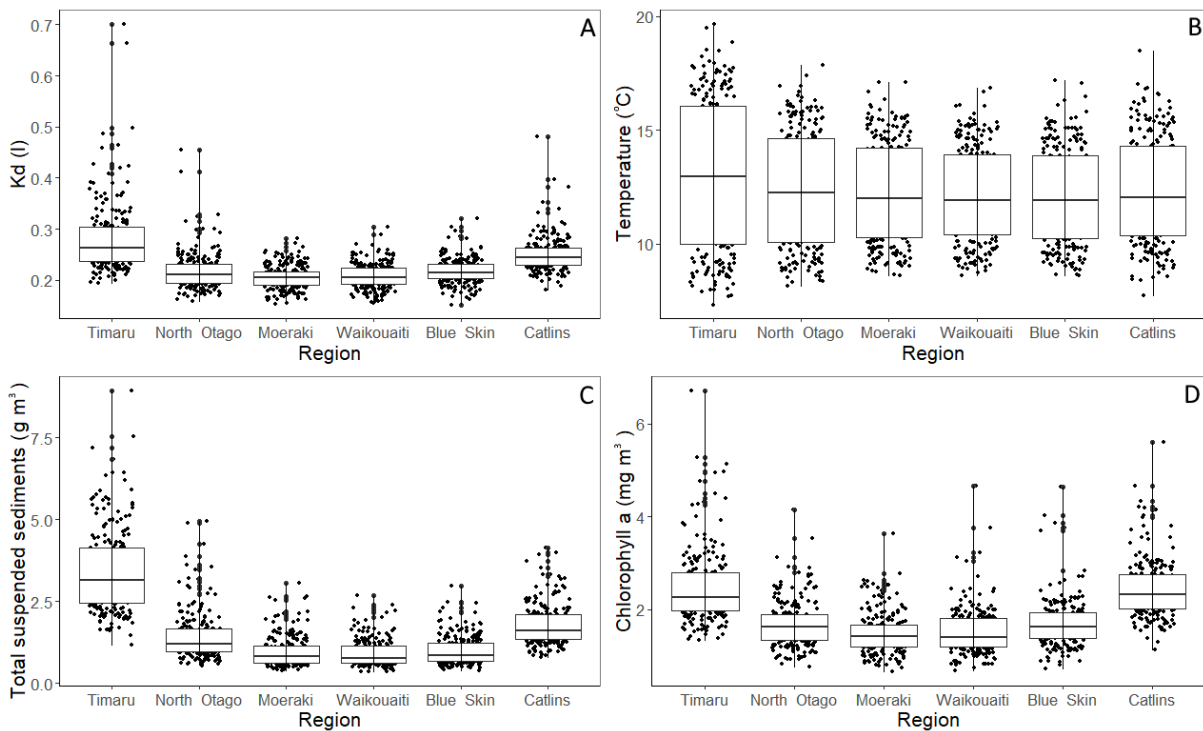


**Figure 3-3: Regional variation in remotely sensed water quality products from 2002–20 across the six study regions.** Water quality products include  $K_d$  (A) or light attenuation (where higher values equal reduced clarity), sea surface temperature (B), total suspended solids (C), and chlorophyll- $a$  (D).

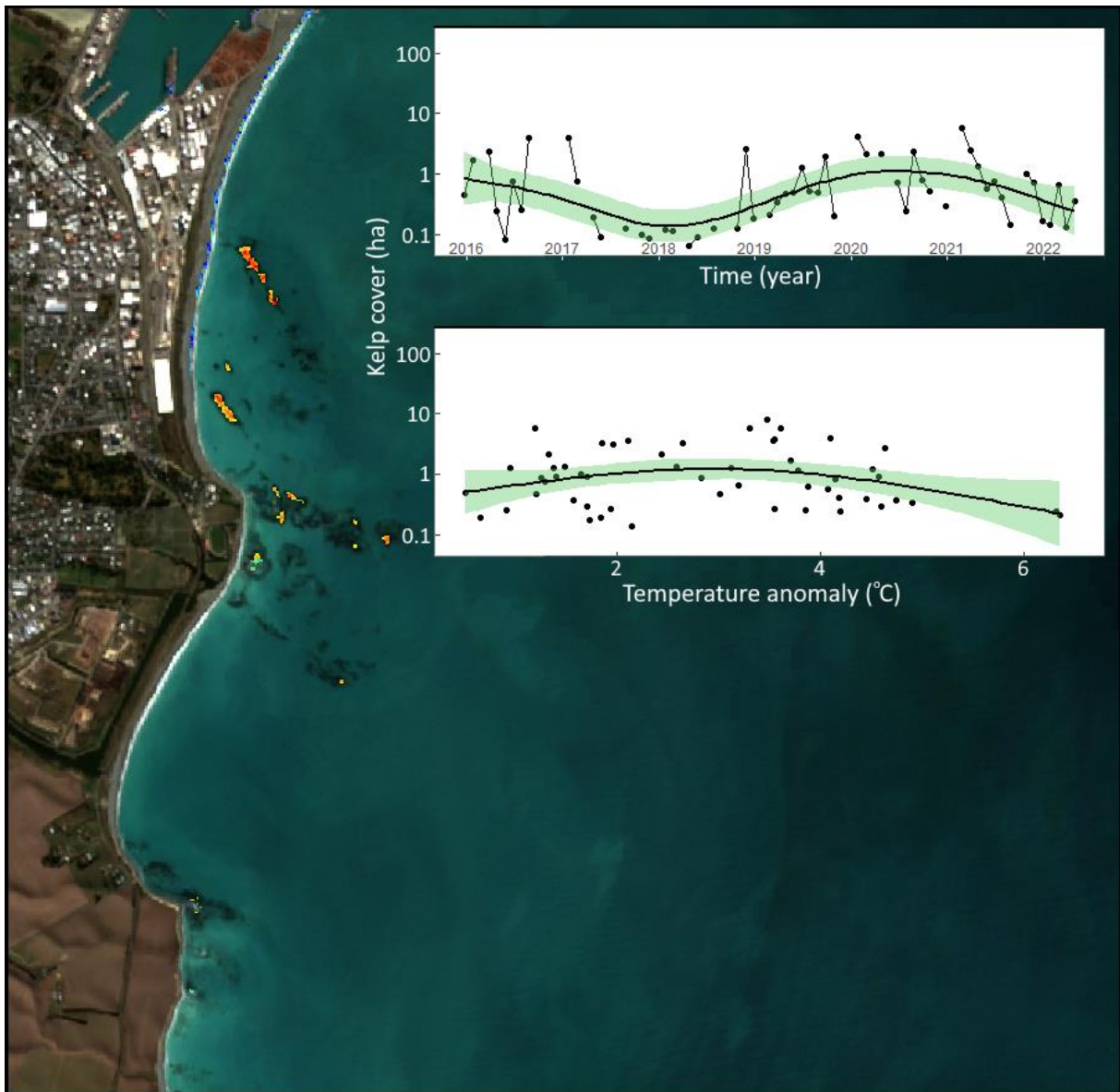


**Figure 3-4: Satellite image of *Macrocyctis* cover in the Timaru region including a timeseries of *Macrocyctis* coverage and the influence of sea surface temperature anomalies on coverage.** Temperature anomalies represent the monthly difference in sea surface temperature to a 20-year timeseries for that location. Trends are plotted using General Additive Models (GAMs). Y-axis is plotted as a logarithmic scale.

*Macrocyctis* in the Timaru region was limited to a small number of patches surrounding Patiti Point and Jacks Point (Figure 3-4). This region is exposed to high levels of sedimentation and had low coverage of *Macrocyctis*. Both low and high temperature anomalies show a negative impact on the coverage of *Macrocyctis*. This region experienced the greatest extremes at each end of the temperature range.

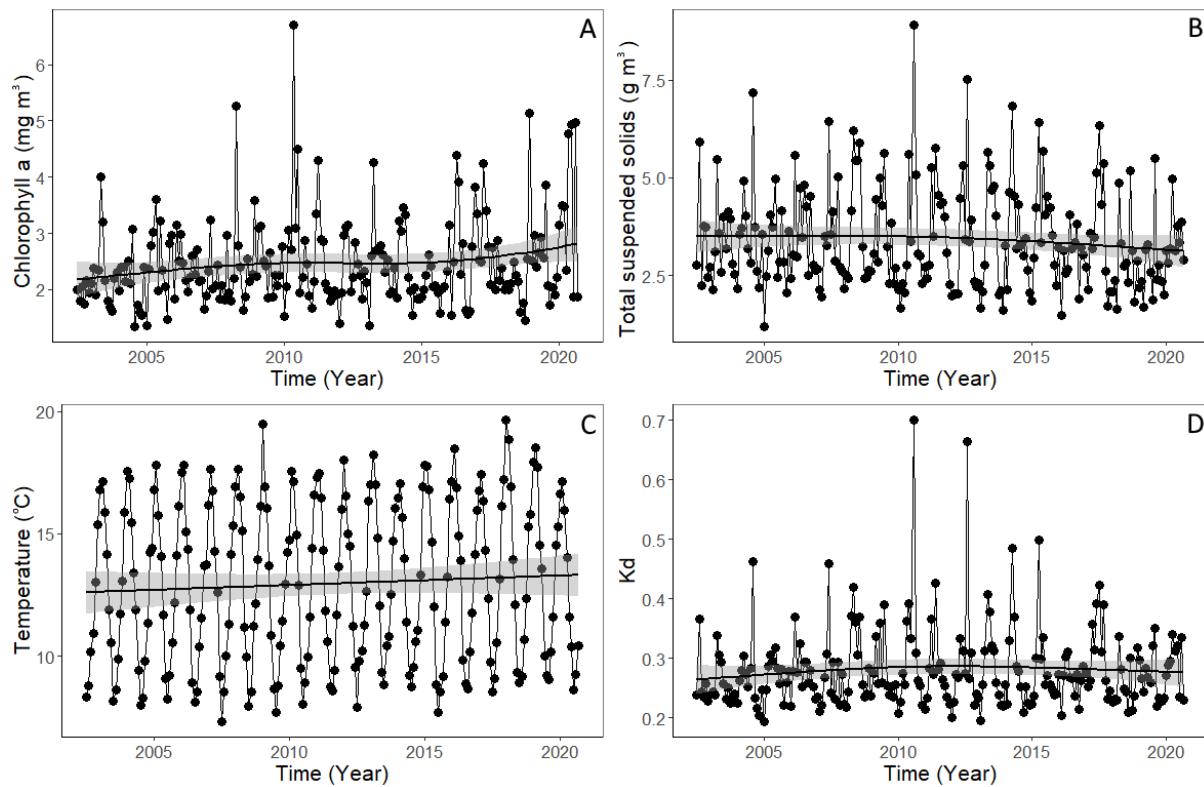


**Figure 3-5: Remotely sensed water quality parameters for the Timaru region.** Water quality products include chlorophyll-*a* (A), total suspended solids (B), sea surface temperature (C), and  $K_d$  or light attenuation (where higher values equal reduced clarity) (D).

Remotely sensed estimates of four water quality products chlorophyll *a*, TSS, sea surface temperature, and  $K_d$  (Figure 3-5) for the Timaru region showed a significant trend of increasing chlorophyll-*a* concentrations over time ( $t = 2.5$ ,  $p = 0.014$ ). Trends for TSS, SST, and  $K_d$  were neutral with no significant changes over time.

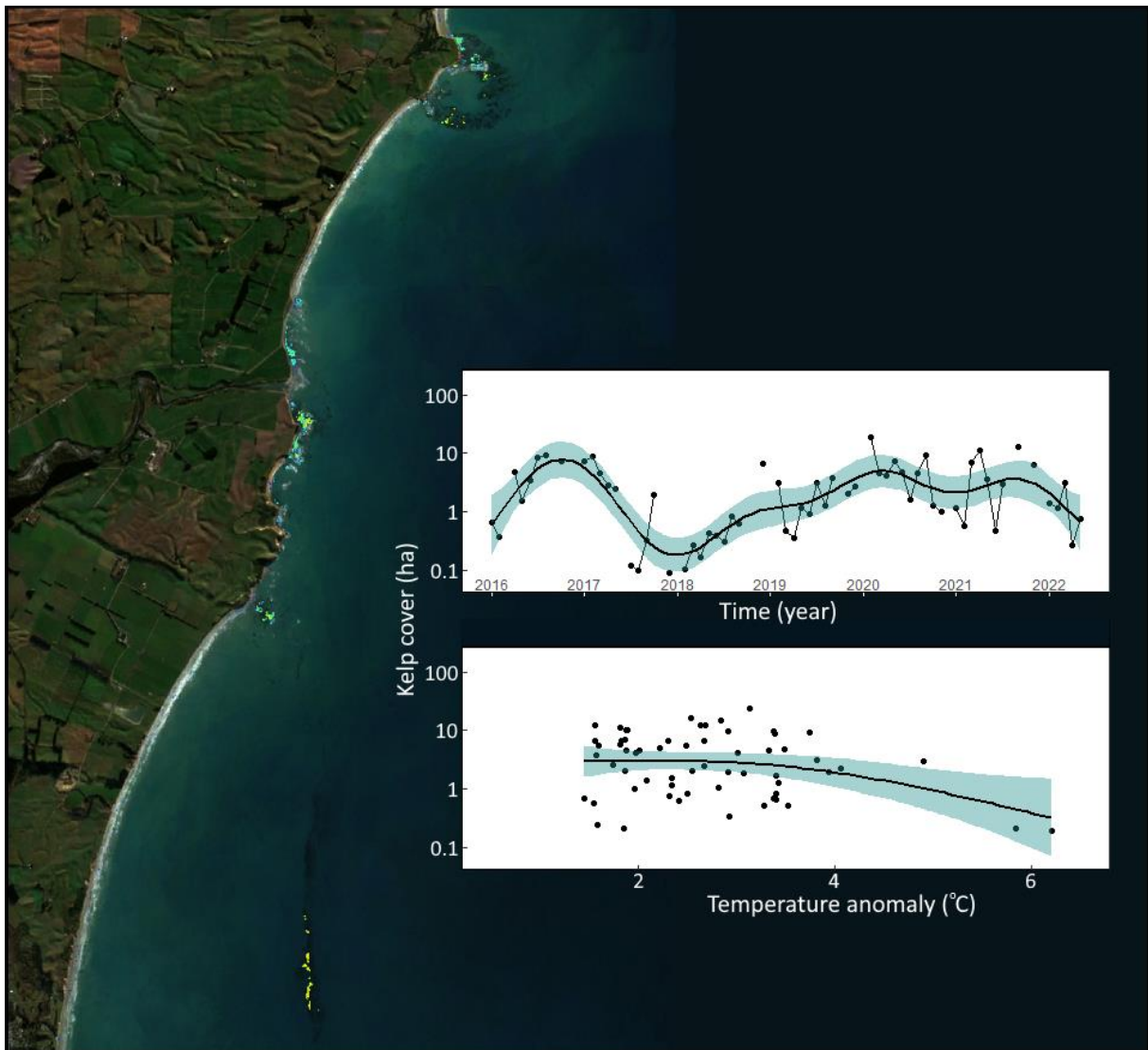


**Figure 3-6: Satellite image of *Macrocyctis* cover in the North Otago region including a timeseries of *Macrocyctis* coverage and the influence of sea surface temperature anomalies on coverage.** Temperature anomalies represent the monthly difference in sea surface temperature to a 20-year timeseries for that location. Trends are plotted using General Additive Models (GAMs). Y-axis is plotted as a logarithmic scale.

North Otago *Macrocyctis* forests were generally characterised by nearshore populations that are exposed to high sediment loads (Figure 3-6). There was a stretch of offshore reef north of the Moeraki Peninsula with detectable *Macrocyctis*, however, this population was frequently not detectable from satellite imagery. The most extreme temperature anomalies had a major influence on *Macrocyctis* coverage in this region.

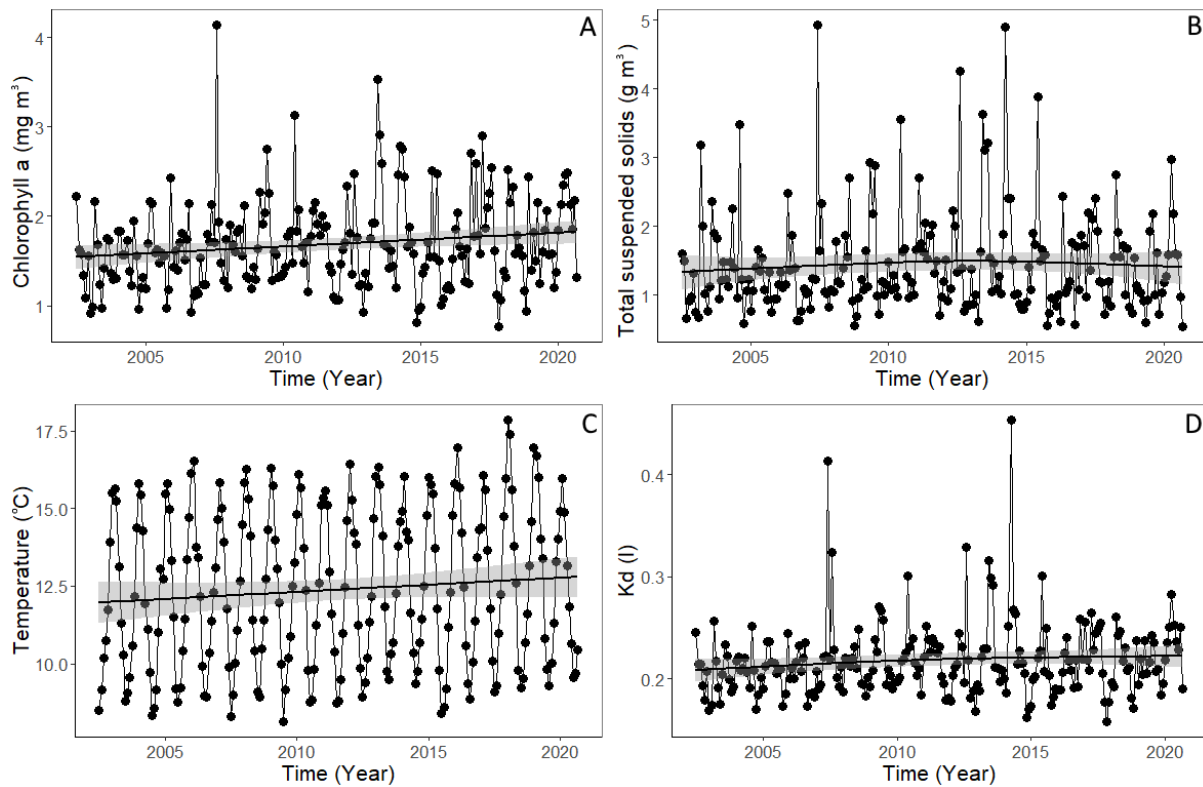


**Figure 3-7: Remotely sensed water quality parameters for the North Otago region.** Water quality products include chlorophyll-*a* (A), total suspended solids (B), sea surface temperature (C), and  $K_d$  or light attenuation (where higher values equal reduced clarity) (D).

Remotely sensed estimates of four water quality products chlorophyll-*a*, TSS, sea surface temperature, and  $K_d$  (Figure 3-7) for the North Otago region showed a trend of increasing chlorophyll-*a* concentrations over time ( $t = 2.4$ ,  $p = 0.016$ ), and near significant increases in  $K_d$  ( $t = 1.6$ ,  $p = 0.1$ ). Trends for TSS and SST were neutral with no significant changes over time.

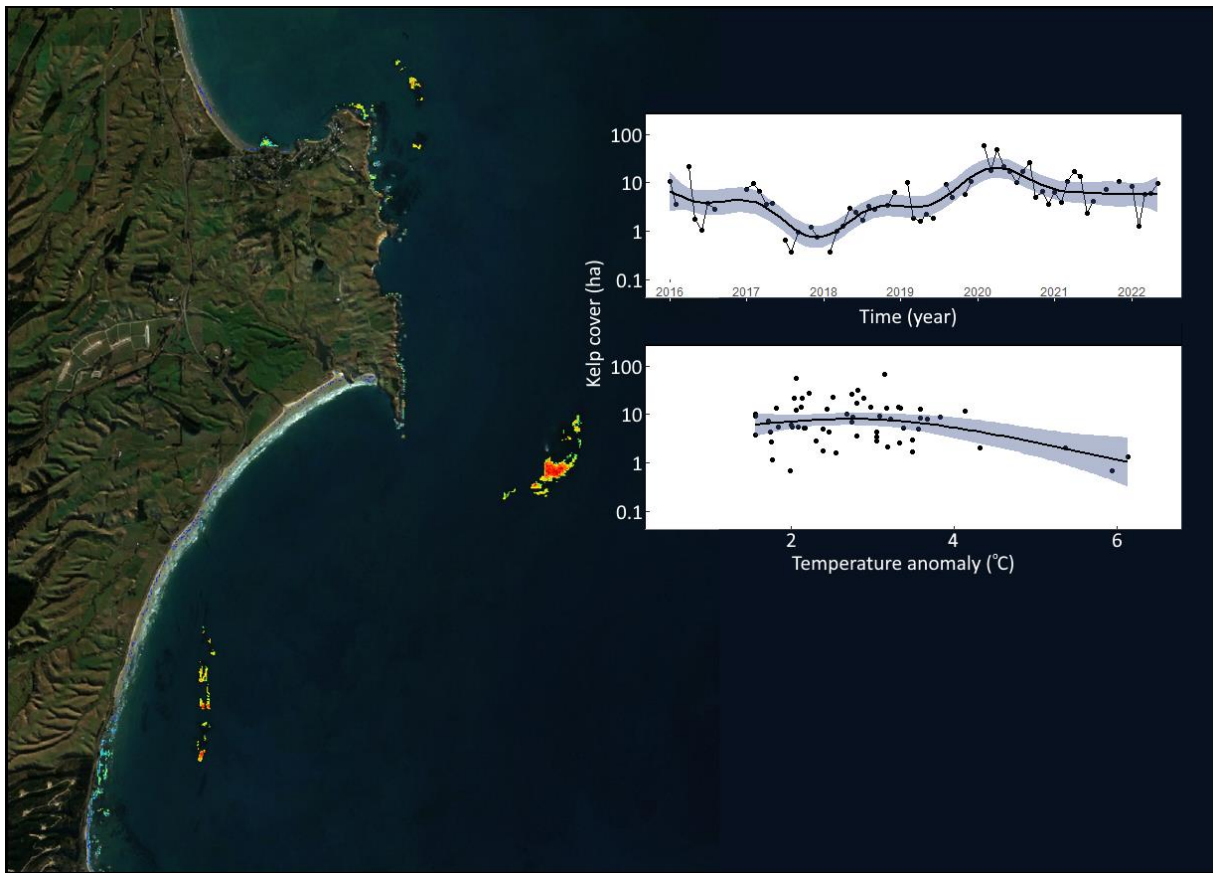


**Figure 3-8: Satellite image of *Macrocyctis* cover in the Moeraki region including a timeseries of *Macrocyctis* coverage and the influence of sea surface temperature anomalies on coverage.** Temperature anomalies represent the monthly difference in sea surface temperature to a 20-year timeseries for that location. Trends are plotted using General Additive Models (GAMs). Y-axis is plotted as a logarithmic scale.

*Macrocyctis* forests surrounding the Moeraki Peninsula were described by several small forests near the northern tip of the Moeraki Peninsula, some offshore reef south of the Peninsula, and a very large population (“Fish Reef”) well offshore from the southern end of the Peninsula (Figure 3-8). The Moeraki region had some of the highest monthly totals of *Macrocyctis* coverage and were dominated by healthy coverage at the “Fish Reef” site. Warm temperature anomalies had a large influence on coverage at this site.

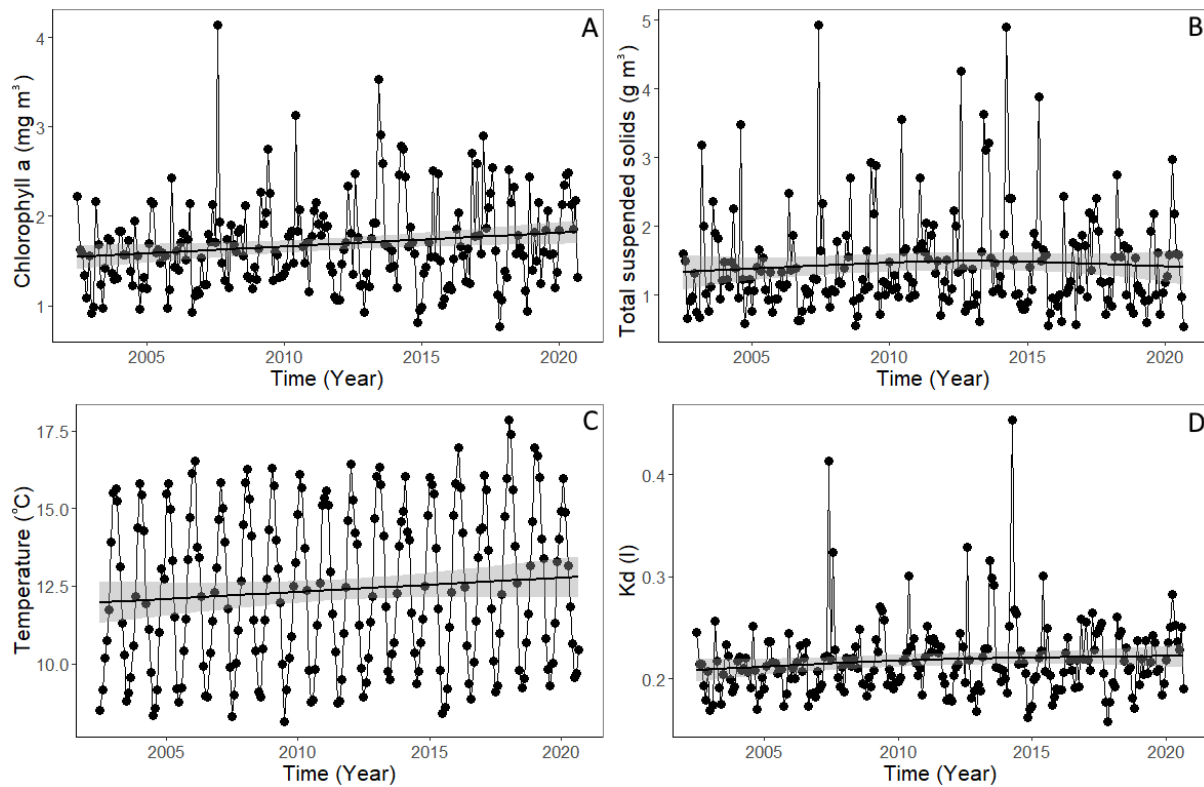


**Figure 3-9: Remotely sensed water quality parameters for the Moeraki region.** Water quality products include chlorophyll-*a* (A), total suspended solids (B), sea surface temperature (C), and  $K_d$  or light attenuation (where higher values equal reduced clarity) (D).

Remotely sensed estimates of four water quality products chlorophyll-*a*, TSS, sea surface temperature, and  $K_d$  (Figure 3-9) for the Moeraki region showed a significant trend of increasing  $K_d$  ( $t = 2.1$ ,  $p = 0.036$ ) and strong trend of increasing SST ( $t = 1.8$ ,  $p = 0.08$ ) over time. Neutral trends for TSS and chlorophyll-*a* were observed.

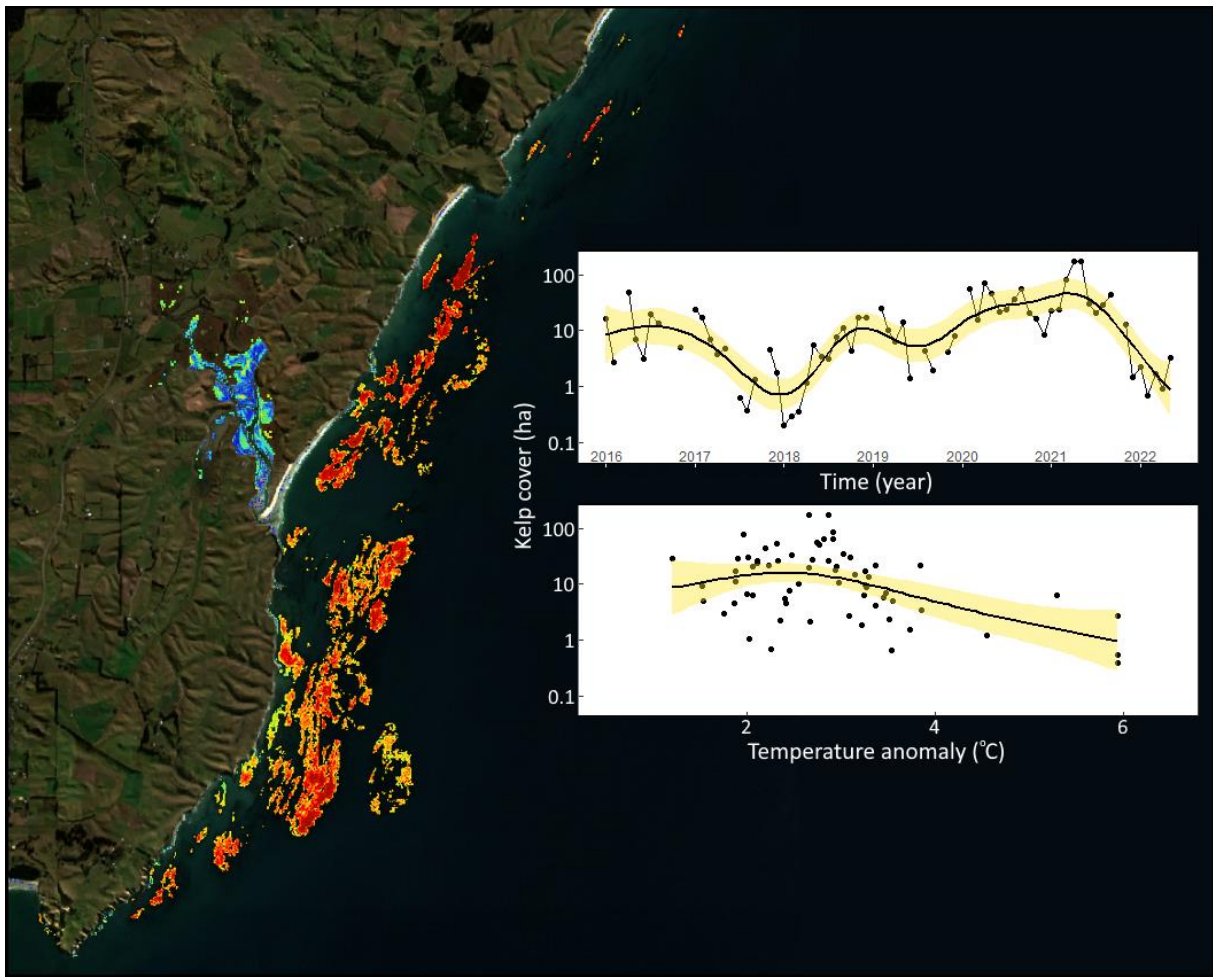


**Figure 3-10: Satellite image of *Macrocyctis* cover in the Waikouaiti region including a timeseries of *Macrocyctis* coverage and the influence of sea surface temperature anomalies on coverage.** Temperature anomalies represent the monthly difference in temperature to a 20-year timeseries for that location. Trends are plotted using General Additive Models (GAMs). Y-axis is plotted as a logarithmic scale.

*Macrocyctis* populations in the Waikouaiti zone were the greatest of any region on the Otago Coast, and possibly represent the biggest populations in New Zealand (Figure 3-10). The forests surrounding Cornish Head are large and extend well offshore. Like other regions, the Waikouaiti region was affected by warm temperature anomalies, but seem to hold up well to minor anomalies (e.g., some of the highest coverage seen during months c. 2°C warmer than the 20-year average).

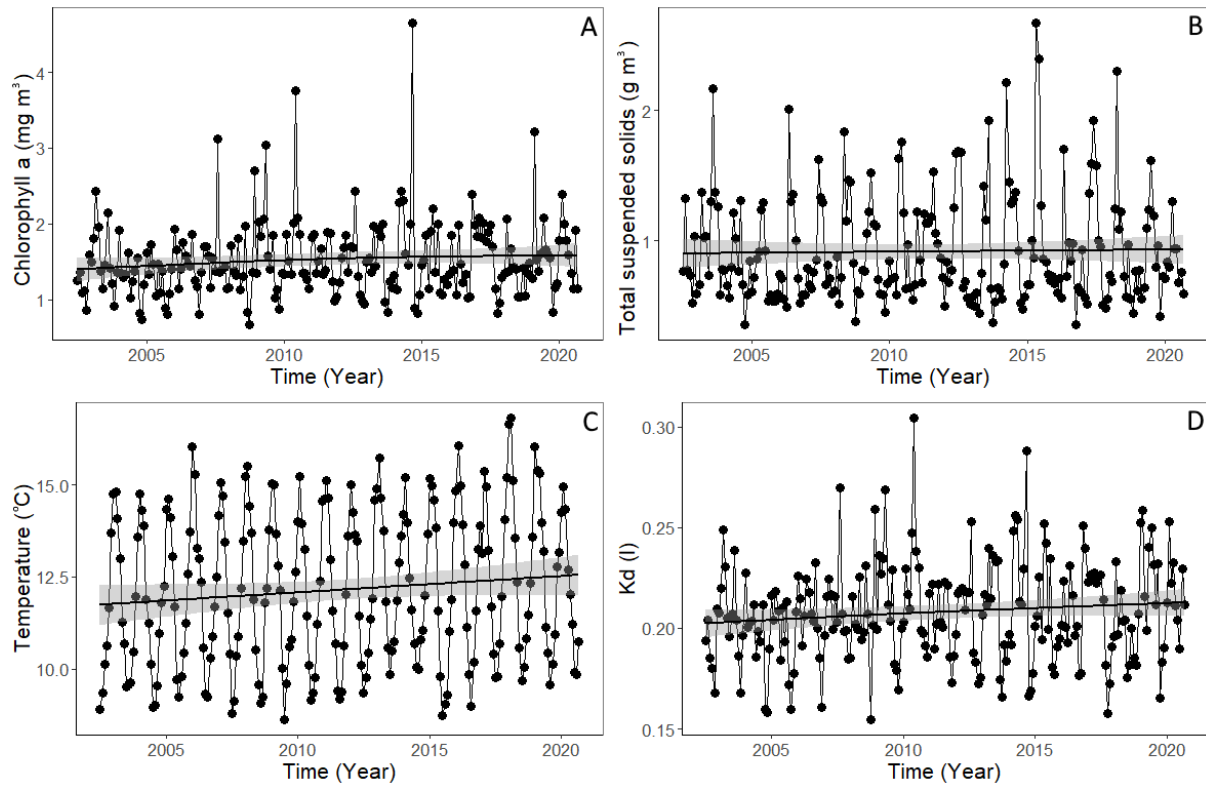


**Figure 3-11: Remotely sensed water quality parameters for the Waikouaiti region.** Water quality products include chlorophyll-*a* (A), total suspended solids (B), sea surface temperature (C), and  $K_d$  or light attenuation (where higher values equal reduced clarity) (D).

Remotely sensed estimates of four water quality products chlorophyll-*a*, TSS, sea surface temperature, and  $K_d$  (Figure 3-11) for the Waikouaiti region showed near significant trends for  $K_d$  ( $t = 1.8$ ,  $p = 0.08$ ) and SST ( $t = 1.7$ ,  $p = 0.09$ ). Neutral trends for chlorophyll-*a* and TSS were observed.

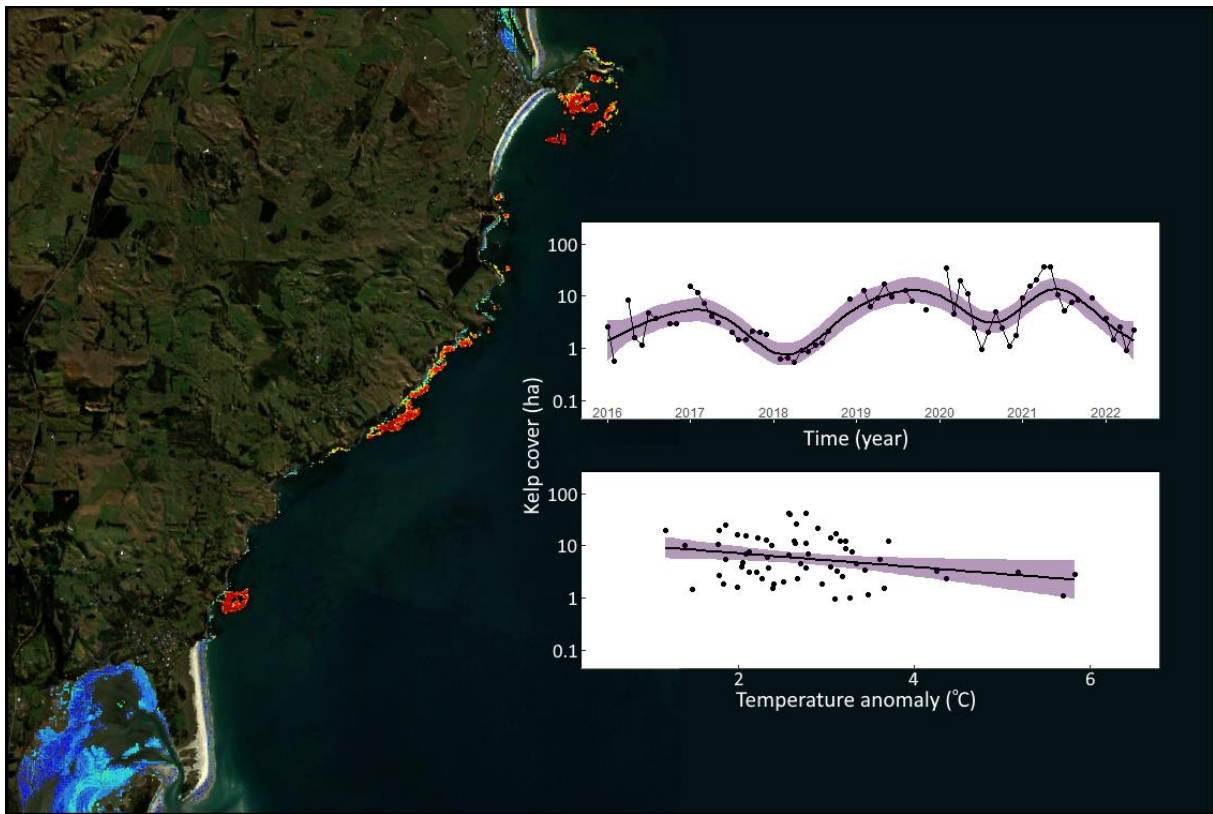


**Figure 3-12: Satellite image of *Macrocyctis* cover in the Blue Skin region including a timeseries of *Macrocyctis* coverage and the influence of sea surface temperature anomalies on coverage.** Temperature anomalies represent the monthly difference in sea surface temperature to a 20-year timeseries for that location. Trends are plotted using General Additive Models (GAMs). Y-axis is plotted as a logarithmic scale.

The Blue Skin Bay Zone had some *Macrocyctis* forests extending slightly offshore at the Karitane Peninsula, but the *Macrocyctis* populations were largely defined by nearshore populations (Figure 3-12). However, there was relatively high coverage of *Macrocyctis* across this region and it was generally similar to the Moeraki region in total coverage. Warm temperature anomalies had a weaker negative effect on coverage than at some other locations.

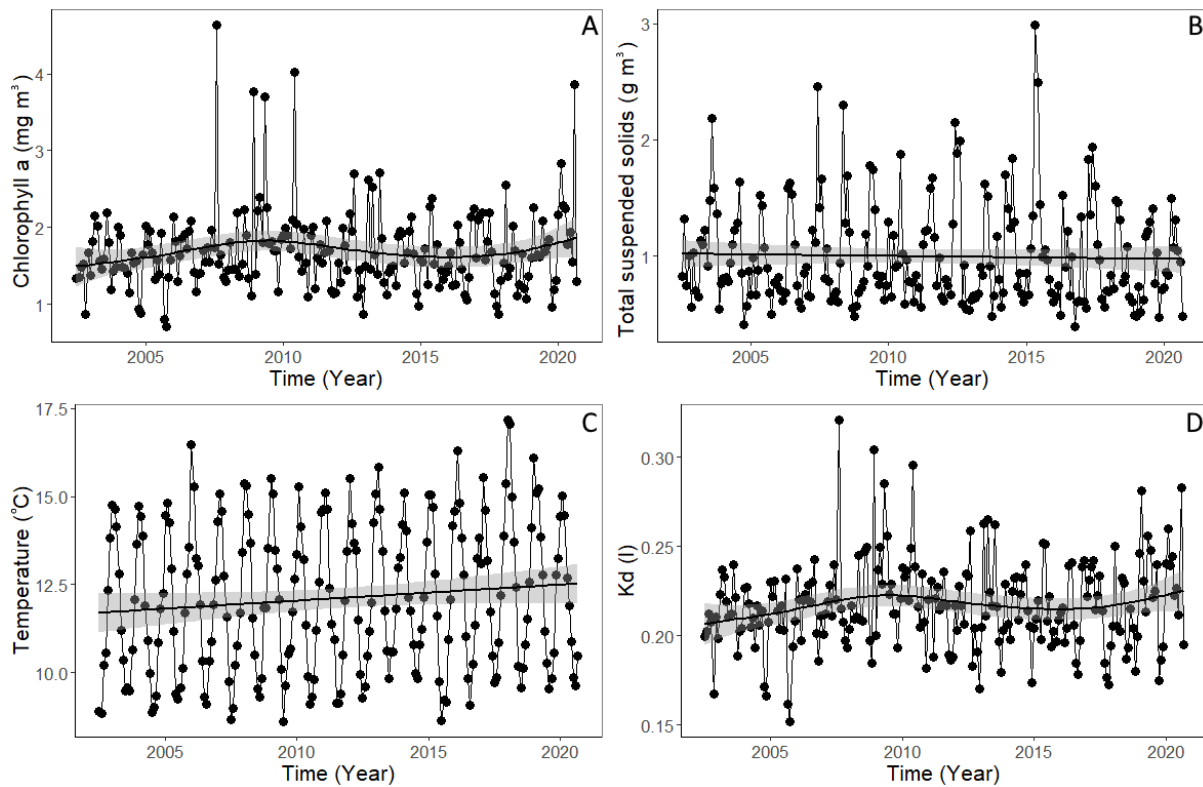


**Figure 3-13: Remotely sensed water quality parameters for the Blue Skin region.** Water quality products include chlorophyll-*a* (A), total suspended solids (B), sea surface temperature (C), and  $K_d$  or light attenuation (where higher values equal reduced clarity) (D).

Remotely sensed estimates of four water quality products chlorophyll-*a*, TSS, sea surface temperature, and  $K_d$  (Figure 3-13) for the Blue Skin region showed a near significant trend of increasing SST ( $t = 1.7$ ,  $p = 0.09$ ) over time. Neutral trends for TSS, chlorophyll-*a*, and  $K_d$  were observed.

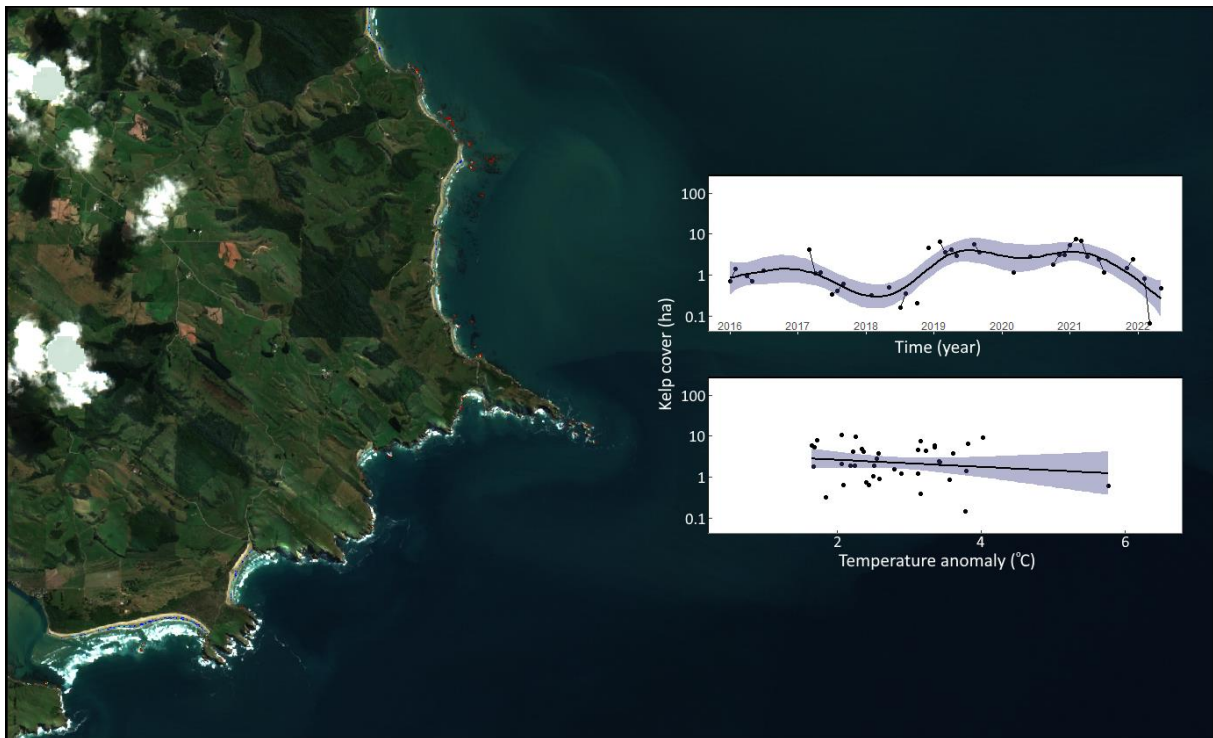


**Figure 3-14: Satellite image of *Macrocyctis* cover in the Catlins region including a timeseries of *Macrocyctis* coverage and the influence of sea surface temperature anomalies on coverage.** Temperature anomalies represent the monthly difference in sea surface temperature to a 20-year timeseries for that location. Trends are plotted using General Additive Models (GAMs). Y-axis is plotted as a logarithmic scale.

*Macrocyctis* forests in the Catlins region were described by only a few locations north of Nugget Point, and just inside the mouth of the Catlins Estuary, where exposure to Southern Ocean swells are reduced (Figure 3-14). These forests were generally small but were often greater in coverage than those observed in Timaru. Warm temperature anomalies had the least influence in the cooler southern region.

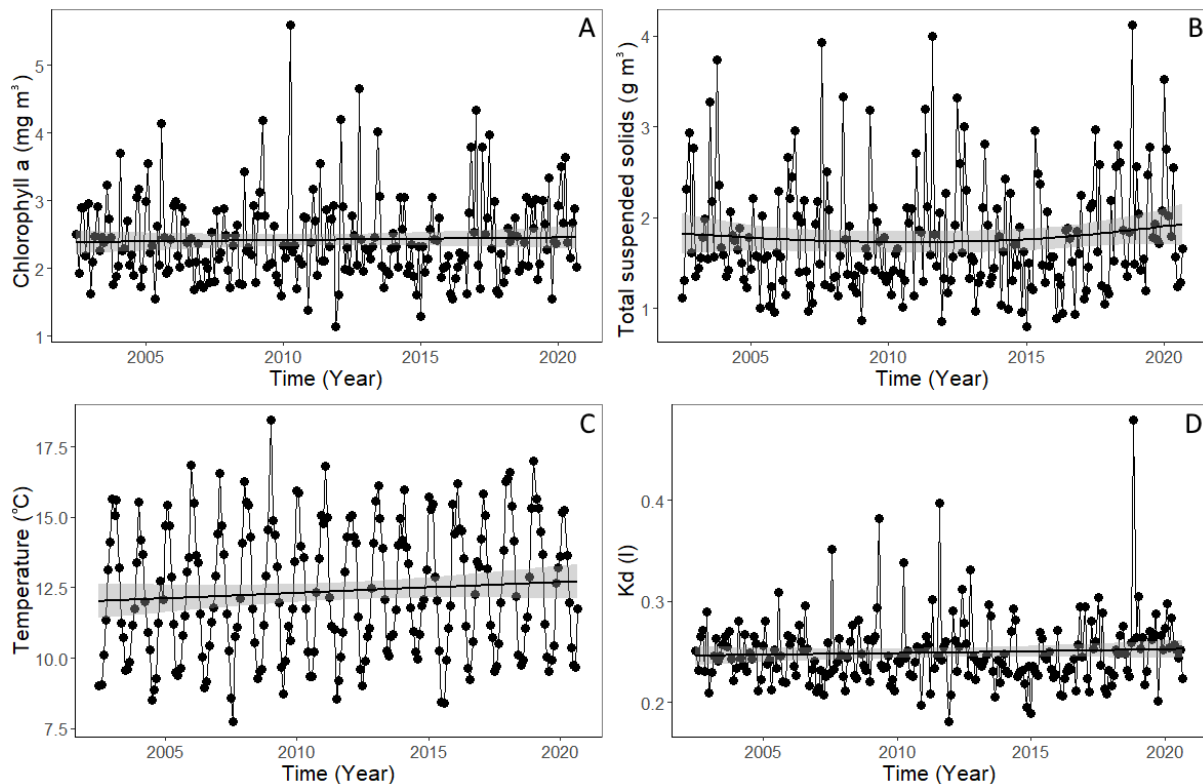


**Figure 3-15: Remotely sensed water quality parameters for the Catlins region.** Water quality products include chlorophyll-*a* (A), total suspended solids (B), sea surface temperature (C), and  $K_d$  or light attenuation (where higher values equal reduced clarity) (D).

Remotely sensed estimates of four water quality products chlorophyll-*a*, total suspended solids, sea surface temperature, and  $K_d$  (Figure 3-15) for the Catlins region showed no meaningful trends in remotely sensed water quality parameters.

### 3.3.2 Summary of *Macrocystis* cover in the Otago region

Overall, the distribution of *Macrocystis* forests across the Otago region (and southern Canterbury) revealed various spatio-temporal trends. *Macrocystis* forests tended to be smaller in size and closer to shore in the northern regions (Timaru Figure 3-4, and North Otago Figure 3-6). Further south towards the Otago Peninsula, *Macrocystis* forests increased in coverage and many large offshore forests were observed (Moeraki Figure 3-8, Waikouaiti Figure 3-10, and Blue Skin Figure 3-12). *Macrocystis* coverage peaked in the Waikouaiti Zone. At the southern extent of the Otago region, small patches of *Macrocystis* were observed near Nugget Point and the mouth of the Catlins Estuary (Figure 3-14). Analysis revealed that sea surface temperature, particularly un-seasonably warm temperatures generally had a negative impact on *Macrocystis* bed coverage. These trends were the most striking for regions with the highest coverage of *Macrocystis* (Figure 3-8; Figure 3-10; Figure 3-12).

## 3.4 Analysis of trends

Combined analysis revealed significant influences of sea surface temperature, suspended sediments, and maximum significant wave height (Table 3-2). While several factors influence *Macrocystis* coverage, increasing temperatures (as shown by temperature anomalies and absolute temperatures) were shown to influence *Macrocystis* coverage across zones (Figure 3-16; Figure 3-17). Warm

temperature anomalies during summer had a negative effect on *Macrocystis* coverage, while warm anomalies in spring and autumn had an initially positive effect, but increasingly negative beyond 2–3°C above average. However, during winter, warm anomalies had a positive influence on *Macrocystis* coverage.

**Table 3-2: Influence of key parameters on *Macrocystis* coverage as estimated by General Additive Models (GAMs).** Overall model (n = 165) has an adjusted r<sup>2</sup> of 0.53, with 57% deviance explained. Significant terms highlighted in bold/italics.

Smooth terms	Edf	Ref.df	F	P-value
SST anomaly * TSS	9.4	27	<b>1.2</b>	<b>&lt;0.0001</b>
SST anomaly	0.9	9	<b>0.8</b>	<b>0.0002</b>
TSS	0.9	9	<b>1.0</b>	<b>&lt;0.0001</b>
Max HS	3.2	9	<b>1.0</b>	<b>0.02</b>

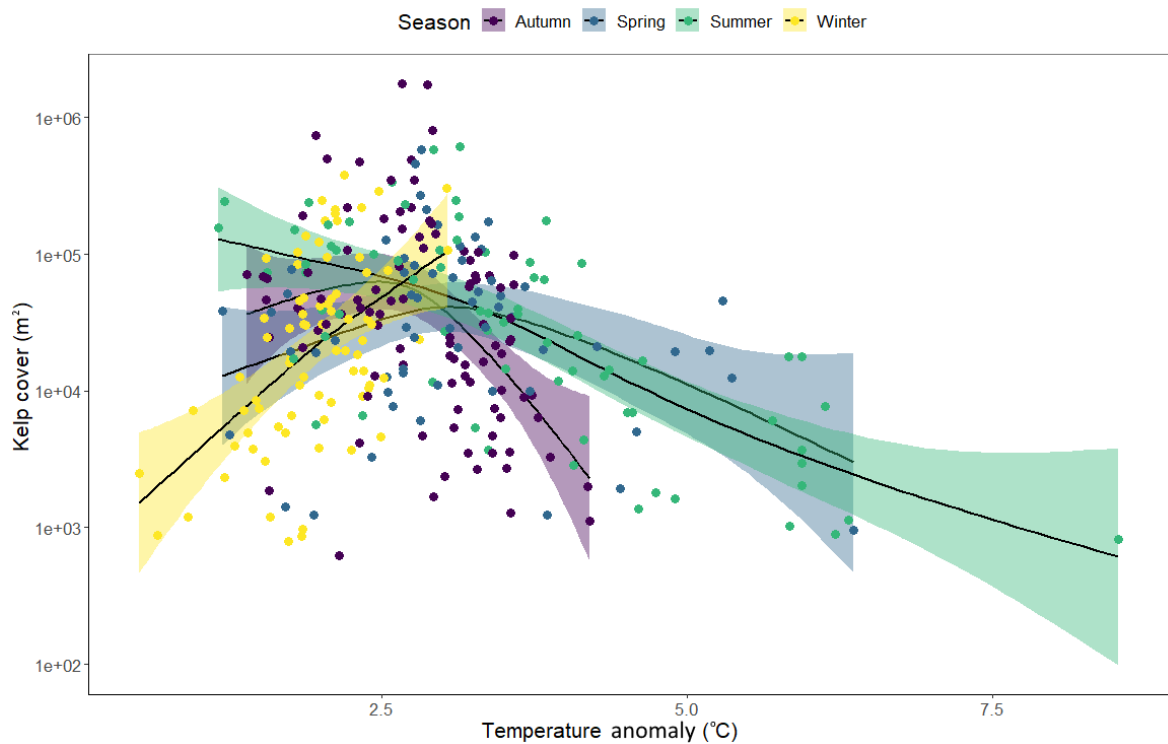


**Figure 3-16: Influence of sea surface temperature anomalies on *Macrocystis* cover between 2016 and 2022.** Trends are plotted separately for each season using General Additive Models (GAMs). Y-axis is a logarithmic scale.

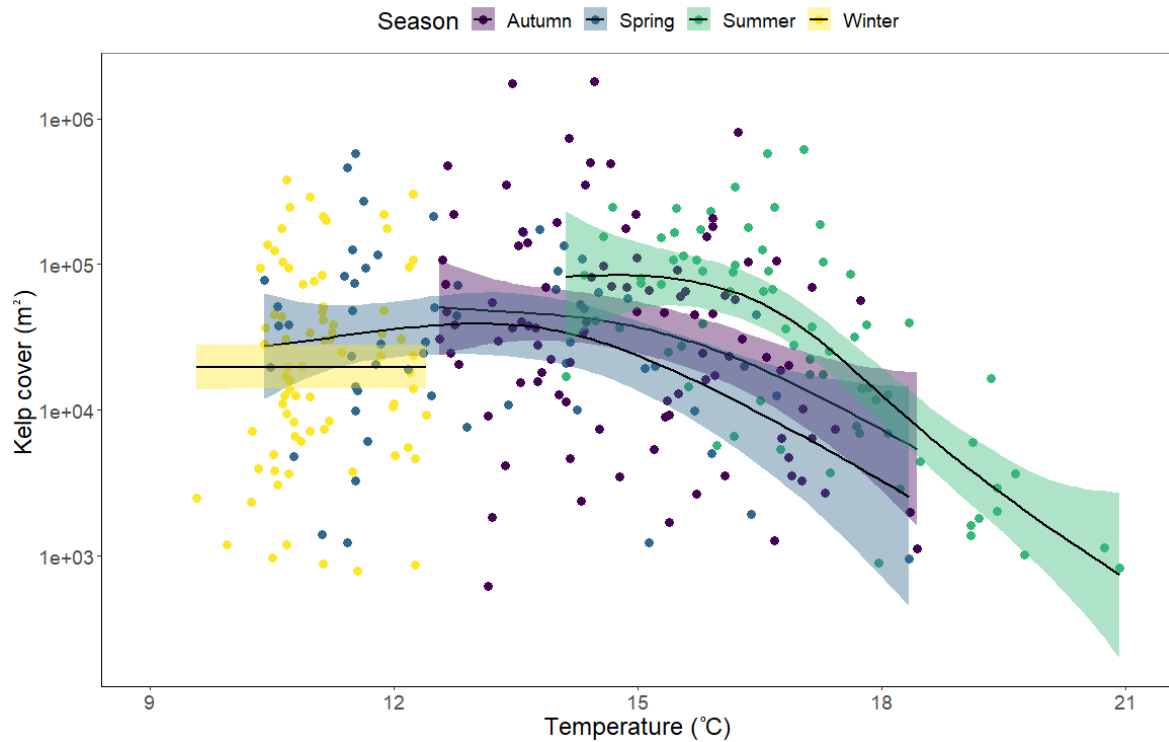


**Figure 3-17: Influence of sea surface temperature anomalies on *Macrocyctis* cover between 2016 and 2022.** Trends are plotted separately for each season using General Additive Models (GAMs). Y-axis is a logarithmic scale.

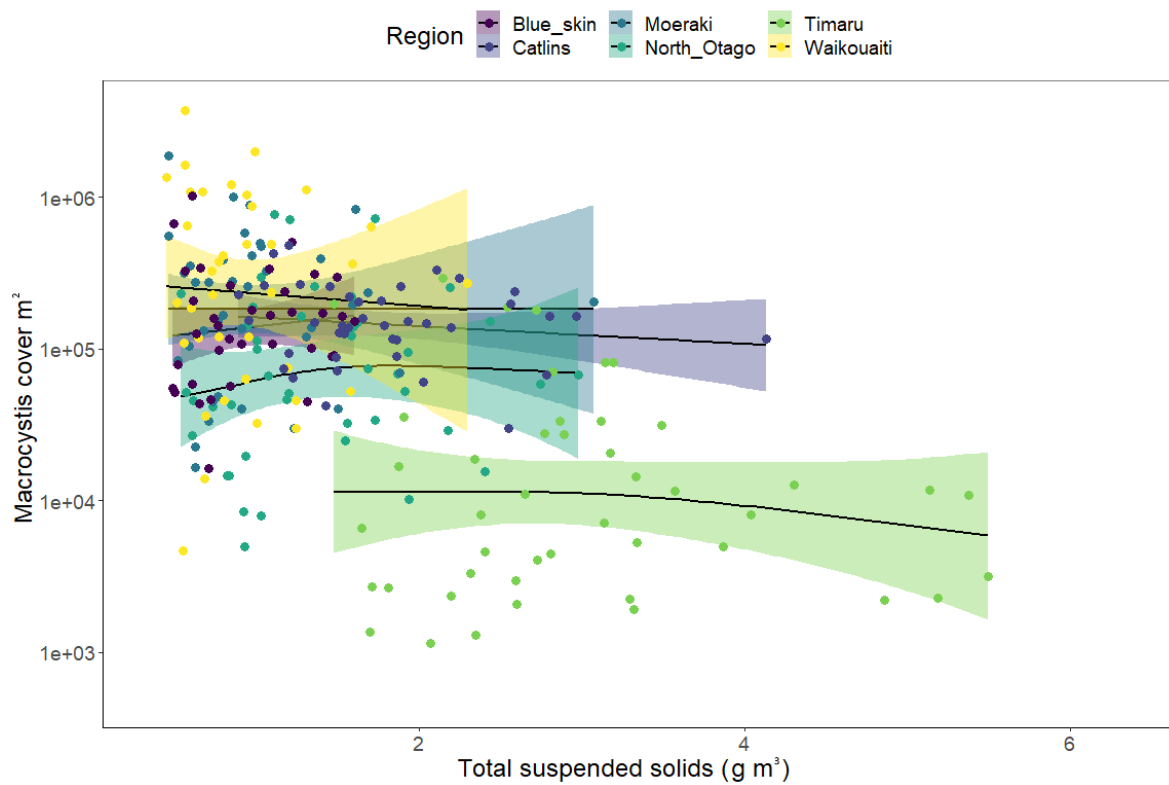


**Figure 3-18: Influence of sediment loads as determined by the particulate backscatter at 555 nm (BBP) on *Macrocyctis* coverage as separated by region.** Trends are plotted separately for each region combined using General Additive Models (GAMs). Y-axis is plotted as a logarithmic scale.

Sites with the lowest range of sediment loads (Waikouaiti and Blue Skin Bay) had neutral or slightly positive relationships between *Macrocystis* cover and TSS, while the other sites had slightly negative relationships (Figure 3-18). Although there was little evidence that temporal variation in suspended sediments within sites caused major declines in *Macrocystis* coverage, variation in sediment loading between sites had a significant influence on observed *Macrocystis* coverage (Figure 3-18). Increasing sediment loads had a negative influence on *Macrocystis* cover, but this was exacerbated by warm temperature (Figure 3-19).

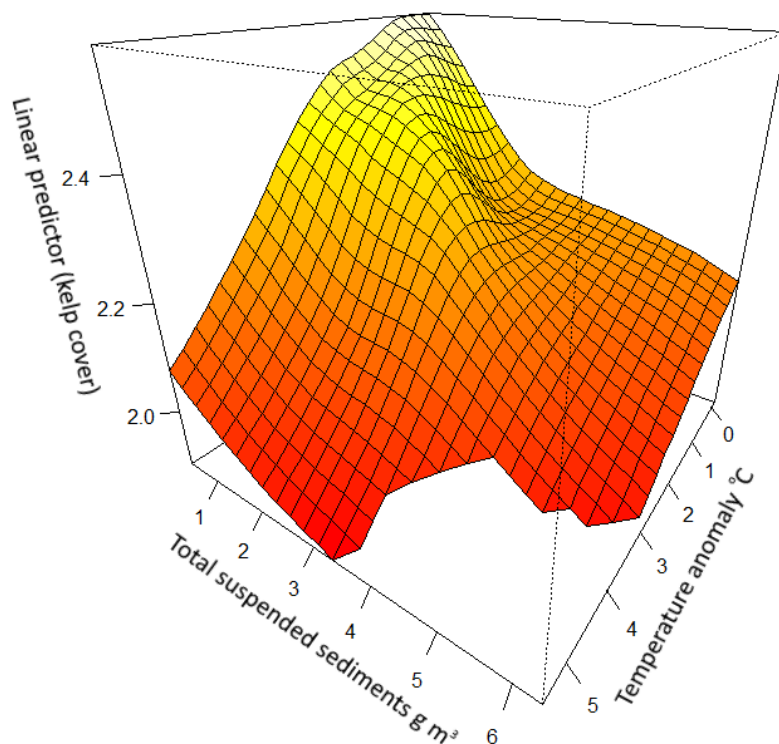


**Figure 3-19: Interactive effects of TSS and temperature anomalies on *Macrocystis* cover as determined by generalised additive models (GAM).**

Using the national bathymetric grid, the cover of *Macrocystis* across the four major *Macrocystis* regions of the North Otago coast were presented across depth bins (from 2016–22). The expected trend was for exponentially decreasing coverage with increasing depth as light becomes limiting. This trend was evident at most sites, however, the Moeraki region had a noticeable increase in coverage at greater depths, particularly at 10-15 m (Figure 3-20). This trend was likely driven by the distribution of rocky reef, with several offshore reefs present in this region. At the Moeraki and Waikouaiti regions there were several instances of *Macrocystis* detected in water depths of 20-30 m. No surface *Macrocystis* was detected at water depths greater than 35 m.

Analysis revealed that increasing temperature anomalies affected *Macrocystis* coverage at all depths and point to a shallowing of the possible habitable depth range of *Macrocystis* (Table 3-3). In addition, elevated sediment loads caused a similar shallowing of depth ranges (Table 3-3).

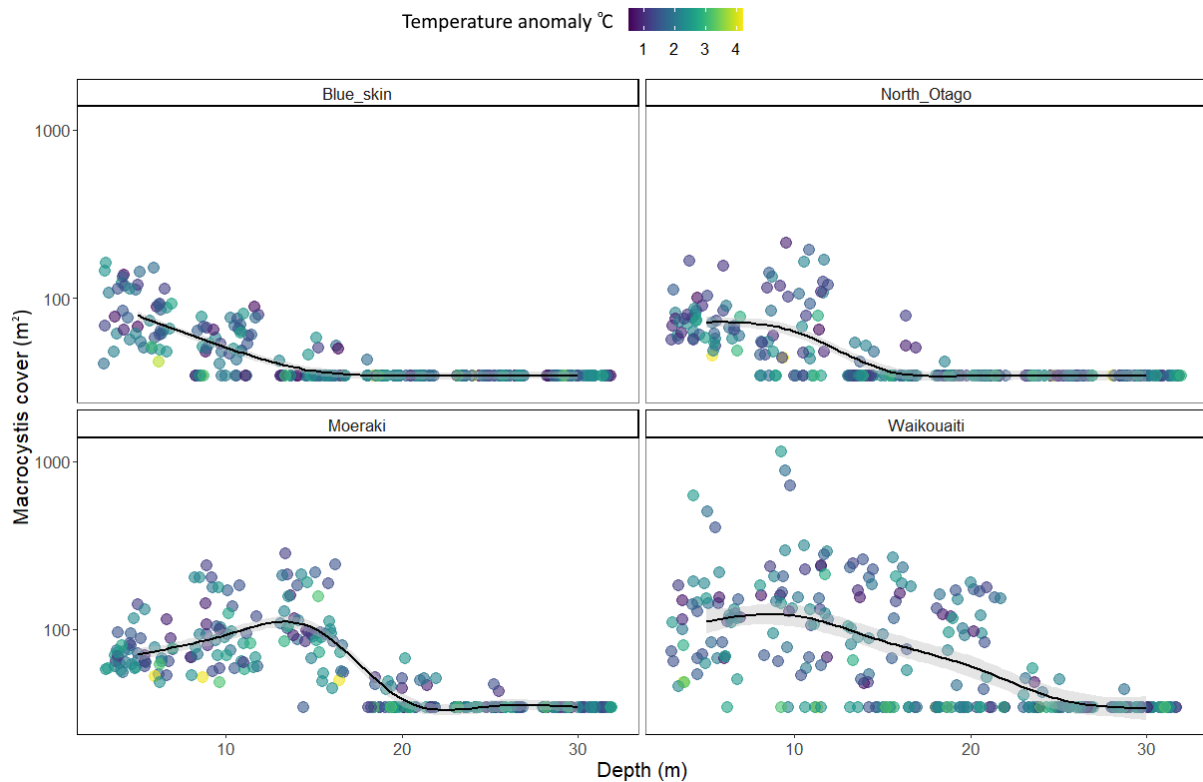


**Figure 3-20: *Macrocyctis* cover across depths between 2016 and 2022.** Sea surface temperature anomalies during each month sampled are presented as a colour scale, with yellow points showing warm anomalies and purple points showing cool anomalies. Y-axis is cube root transformed. Depth estimates are binned into 5m categories, and the points are “jittered” within these bins for visualisation.

**Table 3-3: Influence of key parameters on *Macrocyctis* coverage at multiple depths as estimated by General Additive Models (GAMs).** Overall model (n = 894) has an adjusted  $r^2$  of 0.44, with 64% deviance explained. Significant terms highlighted in bold/italics.

Smooth terms	Edf	Ref.df	F	P-value
Temperature * Depth	15.7	29	<b>6.7</b>	<b>&lt;0.0001</b>
Temperature anomaly	3.3	9	<b>1.9</b>	<b>0.0003</b>
Sediment load	3.8	9	<b>1.4</b>	<b>0.006</b>

## 4 Summary and recommendations

### 4.1 Status of *Macrocystis*

Updated analysis of *Macrocystis* coverage trends has confirmed that warm sea surface temperatures are a major threat to the stability of *Macrocystis* forests in the Otago region. Like previous studies on *Durvillaea* (Thomsen et al. 2019) and *Macrocystis* (Tait et al. 2021), this study shows that warm temperature anomalies, particularly those  $>3\text{--}4^{\circ}\text{C}$ , cause dramatic reductions in the coverage of *Macrocystis*. Despite the severe consequences of marine heatwaves on surface cover of *Macrocystis*, including the summer 2021–22 event, mild summer seasons such as 2020–21 revealed the highest cover of *Macrocystis* over the 6-year period.

Here, I show some of the first evidence that the marine heatwave of summer 2021–22 caused retractions in *Macrocystis* cover. Additionally, I show that the use of a national bathymetric layer can help us identify changes in the depth range that *Macrocystis* can occupy and reveal a shallowing of the habitable depth range during warm conditions.

Alongside warm temperature anomalies, I show that reduced water clarity is an additive stressor to *Macrocystis* forests. While there was little evidence that changes in *Macrocystis* coverage were caused by temporal variations in sediments within regions, there was variation in *Macrocystis* coverage across regions exposed to varying sediment loads. I present a gradient of sediment loading, increasing from Blue Skin Bay to Timaru. Similar gradients exist for the Catlins region, with the Brighton–Taieri coast exposed to high sediment loading which decline towards the southern Catlins region (Figure 4-1).

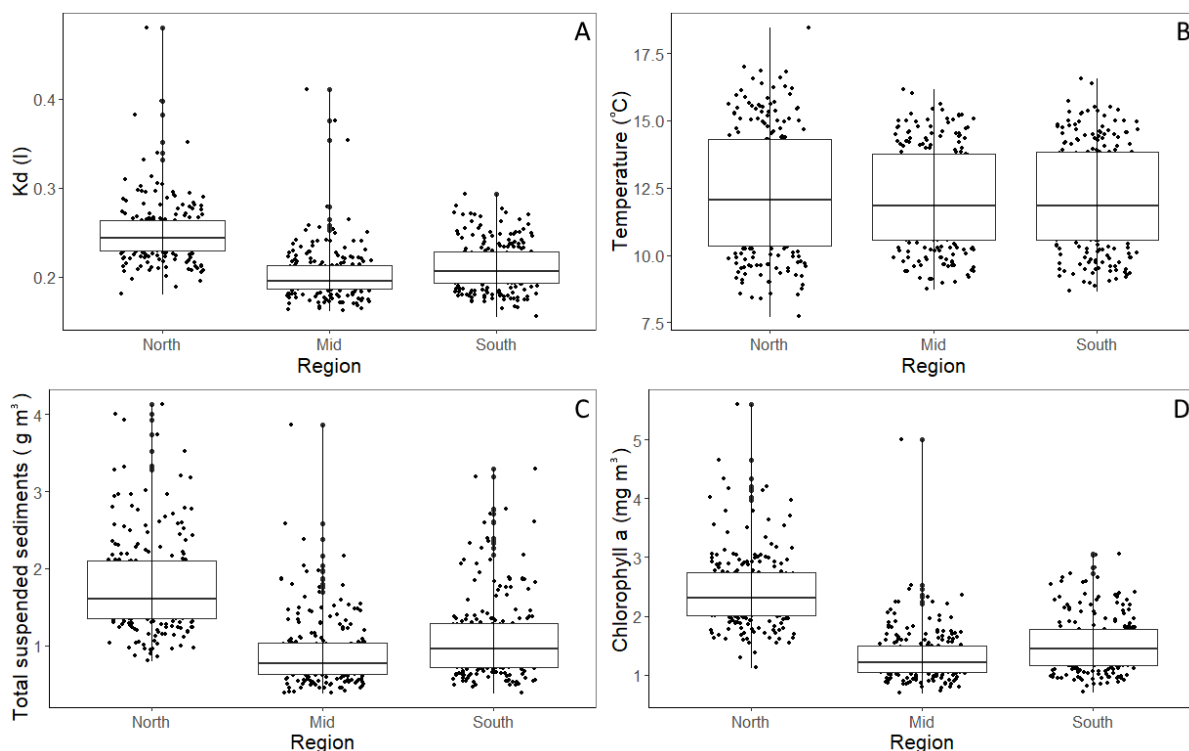


**Figure 4-1:** Remotely sensed water quality products averaged for three zones within the Catlins region, north (near the mouth of the Clutha River), mid (near the Catlins Estuary), and south (near Wapiti (Chaslands) River). Water quality products include Kd (A) or light attenuation (where higher values equal reduced clarity), temperature (B), total suspended solids (C), and chlorophyll-*a* (D).

## 4.2 Future monitoring

To help understand the abundance of deeper-living populations I propose surveying *Macrocystis* populations on deeper rocky reefs at several locations using Remote Operated Vehicles (ROV), drop-cameras and where possible SCUBA (Self Contained Underwater Breathing Apparatus) divers. These methods will also be used at an equal number of shallow reefs adjacent to these deep sites to establish relationships between the two habitats. These measurements will identify uncertainties surrounding passive monitoring methods (i.e., satellites) in assessing *Macrocystis* populations in deeper habitats.

Remote sensing has revealed several areas where *Macrocystis* populations are sporadically present in deeper water. Shifting light availability and increasing frequency of heat-wave events present the greatest threat to *Macrocystis* populations (Tait et al. 2021) and plants at the limits of their depth distribution will likely be the most responsive to subtle water quality shifts. Therefore, I propose establishing in situ validation and calibration of in situ populations in several candidate deep areas (Figure 4-2) to determine depth limitations of *Macrocystis* and fine-tune remotely sensed metrics of ecosystem health.

I propose using georeferenced drop-camera, ROV and SCUBA diver methods to align observations of *Macrocystis* density at the seafloor with satellite observations to examine the accuracy of satellite-based detection methods.

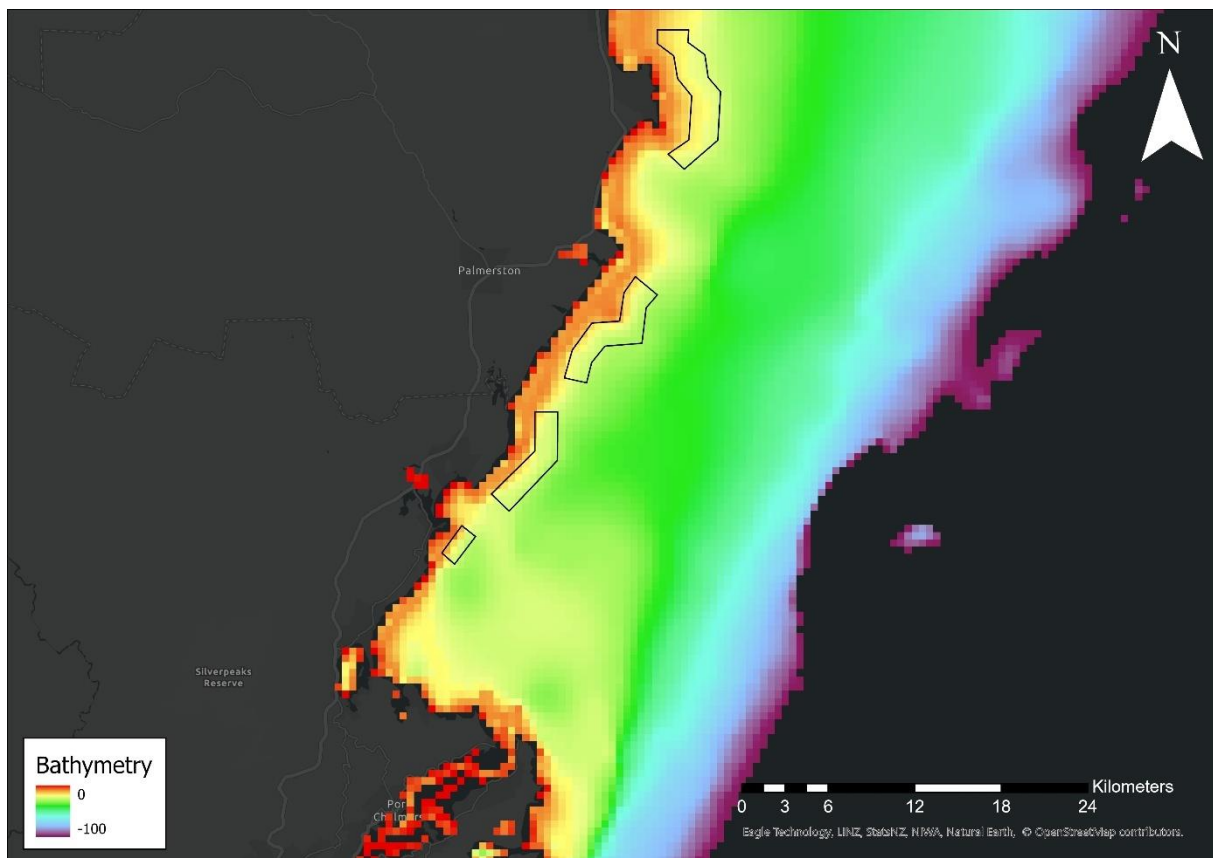


**Figure 4-2: Bathymetry of the Otago Coast from the Otago Peninsula to the Moeraki Peninsula. Candidate regions for in situ validation of deep populations of *Macrocystis* shown by black polygons.**

Although monitoring of *Durvillaea* along some of the northern Otago coastline only began in 2018, there was some evidence that measurements taken during the heatwave affected summer of 2017–18 were lower than the following, non-heat-wave years (Tait 2020). Further evidence is required to understand the consequences of warm water temperatures on *Durvillaea* populations. I propose establishing high-resolution aerial imagery of *Durvillaea* populations in four zones representing a gradient of exposure to discharges from the Clutha River, and gradients of terrestrial land-uses (particularly the relative proximity to agriculture, exotic forests, and native forests) (Figure 4-3). I propose aerial surveys of at least one headland or rocky reef platform in each of the four regions to establish baseline information about *Durvillaea* populations and set up a programme that will help identify sediment related stress on these populations.

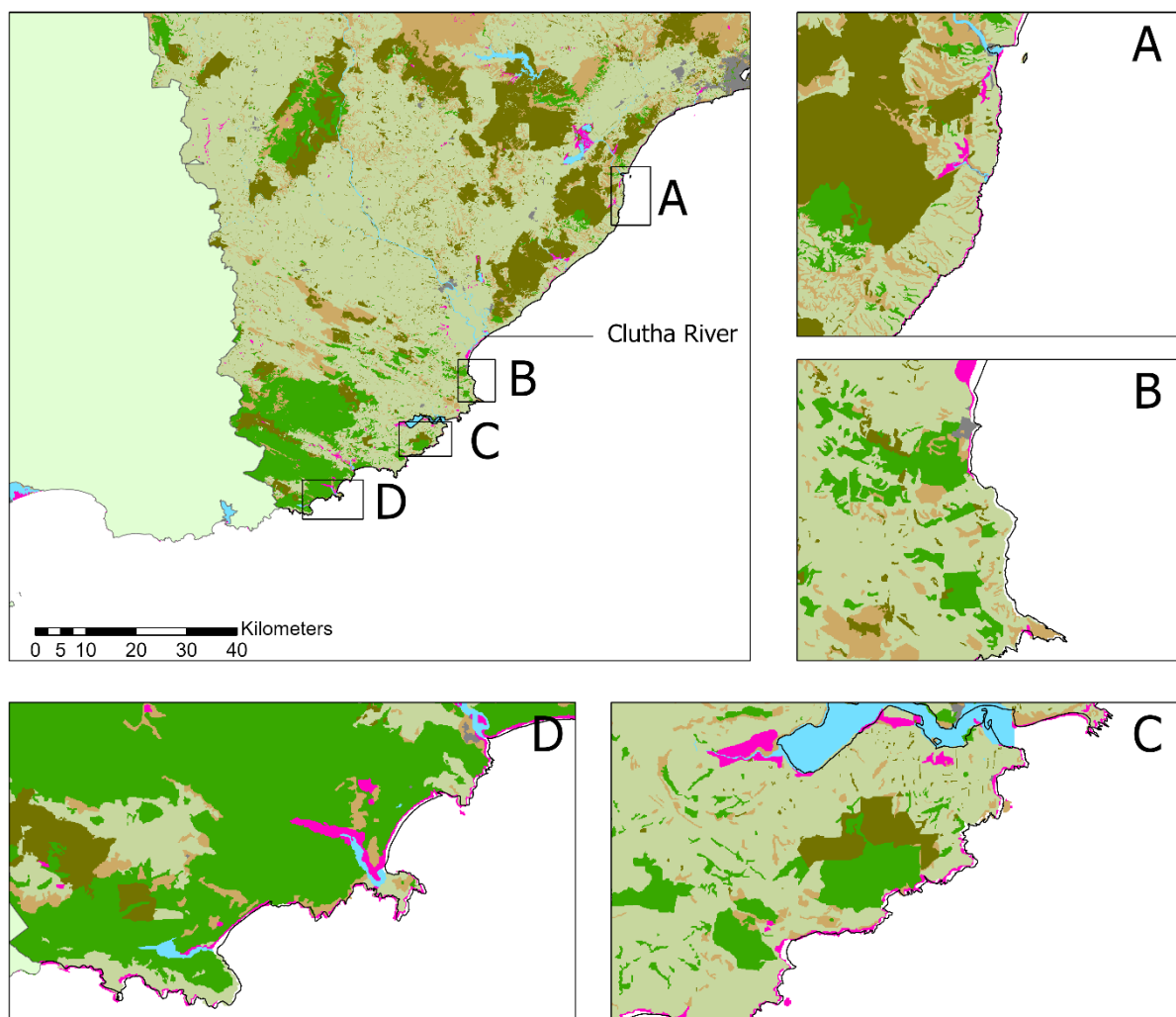


**Figure 4-3: Candidate regions of coastal *Durvillaea* habitats for high-resolution aerial monitoring.** Inset maps show regions of high sediment exposure and low native forest coverage (A); high sediment exposure and moderate native forest cover (B); moderate sediment exposure and moderate native forest cover; and moderate sediment exposure and high native forest cover (D).

## 5 Acknowledgements

I thank Rebecca McGrouther and Port Otago Ltd. for funding data collection in the Blue Skin Bay and Waikouaiti regions and for providing permission to use the data in this report, Steve Copson for

collection of aerial imagery along the Waikouaiti Coast, and Jochen Bind, Stephanie Mangan for assistance analysing aerial and satellite imagery and the SCENZ team (Matt Pinkerton, Mark Gall, Simon Wood and Tilman Steinmetz) for access to satellite-derived water quality products. Thanks to Chris Woods for his constructive reviews of this report.

## 6 Glossary of abbreviations and terms

CHL	Chlorophyll- <i>a</i> : concentrations of phytoplankton as detected by earth-observation satellites. Expressed as milligrams per metre cubed.
GAM	General Additive Model: Statistical analysis of multiple parameters on a single response variable. Unlike general linear models (GLMs), GAMs allow for non-linear trends to be fitted.
Kd or KPAR	Attenuation coefficient for light: low Kd values represent clear water while high values represent turbid water. Expressed as the proportional reduction in light per m of water depth.
NDVI	Normalised Difference Vegetation Index: multi-band index used to define photosynthetic vegetation.
NDWI	Normalised Difference Water Index: multi-band index used to define water bodies.
NIR	Near Infrared Radiation: The radiation wavelengths greater than visible red light. These wavelengths are highly informative of vegetation health.
PAR	Photosynthetically Active Radiation: wavelengths of light required for photosynthetic organisms.
SST	Sea surface temperature: temperature at the sea surface as measured by earth-observation satellites. Expressed as degrees Celsius.
TSS	Total Suspended Solids: suspended sediments (non-biological) within the water column. Expressed as grams per metre cubed.

## 7 References

- Arafeh-Dalmau, N., Montaña-Moctezuma, G., Martinez, J. A., Beas-Luna, R., Schoeman, D. S., Torres-Moye, G. (2019) Extreme marine heatwaves alter kelp forest community near its equatorward distribution limit. *Frontiers in Marine Science*, 6: 499. doi: 10.3389/fmars.2019.00499.
- Bell, T.W., Allen, J.G., Cavanaugh, K.C., Siegel, D.A. (2020) Three decades of variability in California's giant kelp forests from the Landsat satellites. *Remote Sensing of Environment*. 238, 110811.
- Blain, C.O., Hansen, S.C., Shears, N.T. (2021) Coastal darkening substantially limits the contribution of kelp to coastal carbon cycles. *Global Change Biology*, 27(21): 5547–5563.
- Bissett, W.P., Patch, J.S., Carder, K.L., Lee, Z.P. (1997) Pigment packaging and Chl a-specific absorption in high-light oceanic waters. *Limnology and Oceanography*, 42(5):961–968.
- Bricaud, A., Babin, M., Morel, A., Claustre, H. (1995) Variability in the chlorophyll-specific absorption coefficients of natural phytoplankton: analysis and parametrisation. *Journal of Geophysical Research*, 100: 13321–13332.
- D'Archino, R., Piazzì, L. (2021) Macroalgal assemblages as indicators of the ecological status of marine coastal systems: a review. *Ecological Indicators*, 129: p.107835.
- Department of Conservation (2010) *New Zealand Coastal Policy Statement, Policy 11: Indigenous biological diversity (biodiversity)*: 60.
- Dymond, J.R., Shepherd, J.D., Newsome, P.F., Gapare, N., Burgess, D.W., Watt, P. (2012) Remote sensing of land-use change for Kyoto Protocol reporting: the New Zealand case. *Environmental Science & Policy*, 16: 1–8.
- Goff, J. R. (1997) A chronology of natural and anthropogenic influences on coastal sedimentation. *New Zealand Marine Geology*, 138: 105–117. doi: 10.1016/s0025-3227(97)00018-2.
- Gorelick, N., Hancher, M., Dixon, M., Ilyushchenko, S., Thau, D., Moore, R. (2017) Google Earth Engine: Planetary-scale geospatial analysis for everyone. *Remote Sensing Of Environment*, 202: 18–27. doi: 10.1016/j.rse.2017.06.031.
- Kirk, J.T.O. (2011) *Light and photosynthesis in aquatic ecosystems*. Cambridge University Press, Cambridge: 649.
- Layton, C., Coleman, M.A., Marzinelli, E.M., Steinberg, P.D., Swearer, S.E., Vergés, A., Wernberg, T., Johnson, C.R. (2020) Kelp forest restoration in Australia. *Frontiers in Marine Science*, p.74.
- Lee, Z.P., Carder, K.L., Arnone, R.A. (2002) Deriving inherent optical properties from water color: a multi- band quasi-analytical algorithm for optically deep waters. *Applied Optics*, 41: 5755–5772.

- Lee, Z.P., Lubac, B., Werdell, J., Arnone, R. (2009) An Update of the Quasi-Analytical Algorithm (QAA\_v5). Open file online at: [http://www.ioccg.org/groups/Software\\_OCA/QAA\\_v5.pdf](http://www.ioccg.org/groups/Software_OCA/QAA_v5.pdf), 9 pp., 2009
- Lee, Z.P., Du, K.P., Arnone, R. (2005) A model for the diffuse attenuation coefficient of downwelling irradiance. *Journal of Geophysical Research*, 110, c02016, doi:10.1029/2004jc002275.
- Ling, S., Johnson, C., Frusher, S., Ridgway, K. (2009) Overfishing reduces resilience of kelp beds to climate-driven catastrophic phase shift. *Proceedings of the National Academy of Science*, 106: 22341–22345. doi: 10.1073/pnas.0907529106.
- Mabin, C. J., Johnson, C. R., Wright, J. T. (2019) Physiological response to temperature, light, and nitrates in the giant kelp *Macrocystis pyrifera* from Tasmania, Australia. *Marine Ecology Progress Series*, 614: 1–19. doi: 10.3354/meps12900.
- Miller, R. J., Lafferty, K. D., Lamy, T., Kui, L., Rassweiler, A., Reed, D. C. (2018) Giant kelp, *Macrocystis pyrifera*, increases faunal diversity through physical engineering. *Proceeding Royal Society of B: Biological Sciences*, 285: 20172571. doi: 10.1098/rspb.2017.2571.
- Mora-Soto, A., Palacios, M., Macaya, E.C., Gómez, I., Huovinen, P., Pérez-Matus, A., Young, M., Golding, N., Toro, M., Yaqub, M., Macias-Fauria, M. (2020) A high-resolution global map of giant kelp (*Macrocystis pyrifera*) forests and intertidal green algae (Ulvophyceae) with Sentinel-2 imagery. *Remote Sensing*, 12: 694.
- NASA (2018a) Goddard Space Flight Center, Ocean Ecology Laboratory, Ocean Biology Processing Group. Moderate-resolution Imaging Spectroradiometer (MODIS) Aqua 11 $\mu$ m Day/Night Sea Surface Temperature Data; 2018 Reprocessing. NASA OB.DAAC, Greenbelt, MD, USA. doi: data/10.5067/AQUA/MODIS/L3M/SST/2014. [Accessed on 09/22/2020]
- Pinkerton, M.H. (2017) *Satellite remote sensing of water quality and temperature in Manukau Harbour*. NIWA report for Watercare Services Ltd, 2017092WN.
- Pinkerton, M.H., Gall, M., Wood, S., Zeldis, J. (2018) Measuring the effects of mariculture on water quality using satellite ocean colour remote sensing. *Aquaculture Environment Interactions*, 10: 529–545.
- Pinkerton, M.H., Sutton, P.J.H., Wood, S. (2019) *Satellite indicators of phytoplankton and ocean surface temperature for New Zealand*. NIWA Client Report 2018180WNrev1. Prepared for the Ministry for the Environment. Wellington, New Zealand.
- Pinkerton, M., Gall, M., Steinmetz, T., Wood, S. (2021) NIWA Seas, Coasts and Estuaries New Zealand (NIWA-SCENZ): Image services of satellite water quality products for coastal New Zealand. NIWA-Wellington. [https://gis.niwa.co.nz/portal/apps/experiencebuilder/template/?id=9794f29cd417493894df99d422c30ec2&page=page\\_6](https://gis.niwa.co.nz/portal/apps/experiencebuilder/template/?id=9794f29cd417493894df99d422c30ec2&page=page_6)
- Reynolds, R.W., Rayner, N.A., Smith, T.M., Stokes, D.C., Wang, W. (2002) An improved in situ and satellite SST analysis for climate. *Journal of Climate*, 15: 1609–1625.

- Rogers-Bennett, L., Catton, C. (2019) Marine heat wave and multiple stressors tip bull kelp forest to sea urchin barrens. *Science Reports*, 9: 1–9. doi: 10.3354/meps10573.
- Salinger, M. J., Renwick, J., Behrens, E., Mullan, A. B., Diamond, H. J., Sirguyev, P., Smith, R.O., Trought, M.C., Alexander, L., Cullen, N.J., Fitzharris, B.B. (2019) The unprecedented coupled ocean-atmosphere summer heatwave in the New Zealand region 2017/18: drivers, mechanisms and impacts. *Environmental Research Letters*, 14:044023. doi: 10.1088/1748-9326/ab012a.
- Schiel, D. R., Foster, M. S. (2015) *The Biology and Ecology of Giant Kelp Forests*. California: Univ. of California Press.
- Schiel, D.R., Gunn, T.D. (2019) Effects of sediment on early life history stages of habitat-dominating furoid algae. *Journal of Experimental Marine Biology and Ecology*, 516: 44–50.
- Sutton, P.J. (2003) The Southland Current: a subantarctic current. *New Zealand Journal of Marine and Freshwater Research*, 37(3): 645–652.
- Tait, L. W. (2018) *Kelp forest monitoring: Photosynthetically active radiation (PAR) monitoring and kelp community composition during disposal operations*. NIWA Client report, prepared for Port Otago Ltd: 60.
- Tait, L. W. (2019) Giant kelp forests at critical light thresholds show compromised ecological resilience to environmental and biological drivers. *Estuarine, Coastal and Shelf Science* 219: 231–241. doi: 10.1016/j.ecss.2019.02.026.
- Tait, L.W., Bind, J., Charan-Dixon, H., Hawes, I., Pirker, J., Schiel, D. (2019) Unmanned aerial vehicles (UAVs) for monitoring macroalgal biodiversity: comparison of RGB and multispectral imaging sensors for biodiversity assessments. *Remote Sensing*, 11(19): 2332.
- Tait, L.W. (2020) *Rocky reef monitoring: Subtidal and intertidal rocky reef monitoring of the northern Otago Coast*. NIWA Client report, prepared for Port Otago Ltd: 27.
- Tait, L.W., Orchard, S., Schiel, D.R. (2021) Missing the forest and the trees: Utility, limits and caveats for drone imaging of coastal marine ecosystems. *Remote Sensing*, 13(16): p.3136.
- Tait, L.W., Thorat, F., Pinkerton, M.H., Thomsen, M.S., Schiel, D.R. (2021) Loss of giant kelp, *Macrocystis pyrifera*, driven by marine heatwaves and exacerbated by poor water clarity in New Zealand. *Frontiers in Marine Science*, p.1168. doi: 10.3389/fmars.2021.721087
- Thomsen, M. S., Mondardini, L., Alestra, T., Gerrity, S., Tait, L.W., South, P. M., Lilley, S.A., Schiel, D.R. (2019) Local extinction of bull kelp (*Durvillaea* spp.) due to a marine heatwave. *Frontiers in Marine Science*, 6: 84. doi: 10.3389/fmars.2019.00084.
- Timmer, B., Reshitnyk, L.Y., Hessing-Lewis, M., Juanes, F., Costa, M. (2022) Comparing the use of red-edge and near-infrared wavelength ranges for detecting submerged kelp canopy. *Remote Sensing*, 14(9): p.2241.

Udy, J.A., Wing, S.R., Connell-Milne, S.O., Durante, L.M., McMullin, R.M., Kolodzey, S., Frew, R.D. (2019) Regional differences in supply of organic matter from kelp forests drive trophodynamics of temperate reef fish. *Marine Ecology Progress Series*, 621: 19–32.